Journal of Computational and Applied Mathematics 372 (2020) 112721

Contents lists available at ScienceDirect

Journal of Computational and Applied Mathematics

journal homepage: www.elsevier.com/locate/cam

Analysis of an a posteriori error estimator for a variational inequality governed by the Stokes equations☆

Feifei Jing [a], Weimin Han [b,c], Yongchao Zhang [c], Wenjing Yan [c,*]

[a] School of Mathematics and Statistics, and Xi'an Key Laboratory of Scientific Computation and Applied Statistics, Northwestern Polytechnical University, Xi'an 710129, Shaanxi, China
[b] Department of Mathematics, The University of Iowa, Iowa City, IA 52242-1410, USA
[c] School of Mathematics and Statistics, Xi'an Jiaotong University, Xi'an 710049, Shaanxi, China

ARTICLE INFO

Article history:
Received 6 August 2018
Received in revised form 3 December 2019

Keywords:
Stokes equations
Variational inequality
Finite element method
A posteriori error estimator
Reliability and efficiency

ABSTRACT

In this work, a residual type a posteriori error estimator is presented for finite element approximations of a variational inequality arising in hydrodynamics, which is governed by the stationary Stokes equations with a nonlinear slip boundary condition of friction type. Reliability of the estimator is rigorously proved, and efficient error control is analyzed, both are based on an equality problem with a Lagrangian multiplier. And an algorithm of recovering the multiplier is also provided. Numerical results are reported to illustrate the good performance of the estimator in the adaptive solution of the variational inequality, as well as the availability of the multiplier.

1. Introduction

Over the past few decades, the adaptive mesh refinement technique has become an important tool for solving efficiently both linear and nonlinear problems in sciences and engineering. The basis of a successful adaptive procedure is the availability of a reliable and efficient a posteriori error estimator of a numerical solution, which is a computable quantity depending only on the problem data and the numerical solution. A posteriori error analysis for the numerical solution of differential equations started in late 1970s with the seminal work by Babuška and Rheinboldt [1,2]. For comprehensive surveys on existing a posteriori error estimators and adaptive procedures, the reader is referred to [3–5].

A posteriori error analysis of finite element methods for the Stokes equations, for both conforming and nonconforming methods, can be found in numerous publications, and the a posteriori error estimator can be classified into two types: residual type [6–13] and recovery type [14]. Notice that it is more difficult to develop a posteriori error estimator for numerical solutions of variational inequalities due to the inequality feature. Nevertheless, a number of papers can be found on a posteriori error estimation of finite element methods for elliptic variational inequalities, e.g. [15–20] for the obstacle problem, and [21,22] for the frictional contact problem. An a posteriori error estimator of discontinuous Galerkin methods for variational inequalities can be found in [23]. Nonetheless, for the inequality problems in hydrodynamics, most publications provide a prior error estimation, e.g., [24–34], and few work can be found on a posteriori error analysis [35,36].

☆ This work is supported by the Natural Science Foundation of Shaanxi Province (Nos. 2019JQ-173, 2019JM-367), the National Science Foundation under grant DMS-1521684, the National Natural Science Foundation of China (Nos. 11971377, 11701451, 51790512) and the Fundamental Research Funds for the Central Universities (No. 31020180QD078).

* Corresponding author.
E-mail addresses: ffjing@nwpu.edu.cn (F. Jing), weimin-han@uiowa.edu (W. Han), yoczhang@126.com (Y. Zhang), wenjingyan@mail.xjtu.edu.cn (W. Yan).

https://doi.org/10.1016/j.cam.2020.112721
0377-0427/

In this paper, we consider a posteriori error estimation of finite element method for solving a variational inequality of the second kind, which is governed by the Stokes equations with a nonlinear slip boundary condition of friction type. A residual type a posteriori error estimator is proposed and studied. The derivation of the a posteriori error estimate is based on the use of a Lagrangian multiplier which formally turns the inequality into an equation. The reliability of the error estimator is proved in the sense that the estimator is an upper bound for the actual error, and efficiency is also analyzed that the error estimator as a lower bound plus some higher order terms as well as a term reflecting the approximation of the Lagrangian multiplier. Numerical examples are given on the good performance of the error estimator in adaptive solution of the variational inequality. The techniques used in this paper can also be applied to analyze the gradient recovery type error estimators combined with the standard argument of gradient recovery type error analysis for the Stokes problem [37–39].

The rest of this paper is organized as follows. In Section 2 we introduce the variational inequality problem for the Stokes equations and state some results on the variational inequality. Section 3 contains the finite element method setting and the posteriori error estimator of the residual type. In Section 4, we prove the reliability of the estimator, as well as show the analysis of the efficiency. An adaptive algorithm and an iterative algorithm are provided in Section 5, after which some numerical results are presented to show the performance of the adaptive procedure.

2. The variational inequality governed by Stokes equations

We first describe the physical setting of the variational inequality arising in hydrodynamics. For definiteness, we focus on the two-dimensional case and comment that the results can be extended to the three-dimensional case. Let $\Omega \subset \mathbb{R}^2$ be an open bounded convex polygon. We assume $\partial\Omega$ is smooth and split into two nonempty open part Γ_D and Γ_S, with $\partial\Omega = \overline{\Gamma}_D \cup \overline{\Gamma}_S$, $\overline{\Gamma}_D \cap \overline{\Gamma}_S = \emptyset$. Let $\mathbf{n} = (\mathrm{n}_1, \mathrm{n}_2)^T$ be the unit outward normal on the boundary Γ_S, and let $\boldsymbol{\tau}$ be the unit tangent vector obtained by rotating $\mathbf{n}$ counterclockwise for 90°. Then if $\mathbf{v}$ is a vector defined on the boundary, we write $\mathrm{v}_{\mathbf{n}} = \mathbf{v} \cdot \mathbf{n}$ for its normal component, and $\mathbf{v}_{\boldsymbol{\tau}} = \mathbf{v} - \mathrm{v}_{\mathbf{n}}\mathbf{n}$ for its tangential component.

Consider the following Stokes equations with a nonlinear slip boundary condition of friction type

$$-\nu\Delta\mathbf{u} + \nabla p = \mathbf{f}, \quad \mathrm{div}\,\mathbf{u} = 0 \quad \text{in } \Omega, \tag{2.1}$$

$$\mathbf{u} = \mathbf{0} \quad \text{on } \Gamma_D, \tag{2.2}$$

$$\mathrm{u}_{\mathbf{n}} = 0, \quad |\boldsymbol{\sigma}_{\boldsymbol{\tau}}| \le g, \quad \boldsymbol{\sigma}_{\boldsymbol{\tau}} \cdot \mathbf{u}_{\boldsymbol{\tau}} + g|\mathbf{u}_{\boldsymbol{\tau}}| = 0 \quad \text{on } \Gamma_S, \tag{2.3}$$

where $\mathbf{u}$ is the fluid velocity, p is the pressure, $\nu > 0$ is the constant viscosity, $\mathbf{f}$ is a given external force. The quantity $\boldsymbol{\sigma}_{\boldsymbol{\tau}}(\mathbf{u}) = \nu\frac{\partial \mathbf{u}_{\boldsymbol{\tau}}}{\partial \mathbf{n}}$ is the tangential component of the stress vector defined on Γ_S. The positive function $g : \Gamma_S \to (0, \infty)$ is called the threshold slip or barrier function.

The second and third relations in (2.3) are equivalent to the following implications:

$$|\boldsymbol{\sigma}_{\boldsymbol{\tau}}| < g \Rightarrow \mathbf{u}_{\boldsymbol{\tau}} = \mathbf{0} \text{ and } \mathbf{u}_{\boldsymbol{\tau}} \neq \mathbf{0} \Rightarrow \boldsymbol{\sigma}_{\boldsymbol{\tau}} = -g\frac{\mathbf{u}_{\boldsymbol{\tau}}}{|\mathbf{u}_{\boldsymbol{\tau}}|}.$$

Note that if $g \equiv 0$, then (2.3) reduces to the ordinary slip boundary condition: $\mathrm{u}_{\mathbf{n}} = 0$ and $\boldsymbol{\sigma}_{\boldsymbol{\tau}} = \mathbf{0}$. This type of boundary conditions was first introduced by Fujita in [40] for applications in the blood flow in a vein of an arterial sclerosis patient, and flow through a canal with its bottom covered by sherbet of mud and pebbles.

We now list some notation used in this paper. For any open subset ω of Ω with a Lipschitz boundary $\partial\omega$, we denote by $H^m(\omega)$, $L^2(\omega)$ and $L^2(\partial\omega)$ the usual Sobolev and Lebesgue spaces with the canonical norms $\|\cdot\|_{m,\omega}$, $\|\cdot\|_{0,\omega}$, $\|\cdot\|_{0,\partial\omega}$, $m \ge 0$. For $\omega = \Omega$, we will drop the subscript Ω in expressing these norms. Throughout the paper, the boldface symbols denote vector-valued quantities and the letter C denotes a generic positive constant independent of the mesh size. We will also need the following spaces

$$H_0^1(\Omega) = \{v \in H^1(\Omega) : v|_{\partial\Omega} = 0\}, \quad L_0^2(\Omega) = \{q \in L^2(\Omega) : \int_\Omega q = 0\}.$$

Then we introduce

$$\mathbf{V} = \{\mathbf{v} \in [H^1(\Omega)]^2 : \mathbf{v}\,|_{\Gamma_D} = \mathbf{0}, \mathrm{v}_{\mathbf{n}}\,|_{\Gamma_S} = 0\}, \quad Q = L_0^2(\Omega), \quad \mathbf{Y} = [L^2(\Omega)]^2, \quad \boldsymbol{\Lambda} = \mathbf{L}^\infty(\Gamma_S).$$

We also recall some basic results in the study of the boundary value problem (2.1)–(2.3) [41,42]. A weak form of the considered problem is the following variational inequality: find $(\mathbf{u}, p) \in \mathbf{V} \times Q$ such that

$$a(\mathbf{u}, \mathbf{v} - \mathbf{u}) - d(\mathbf{v} - \mathbf{u}, p) + j(\mathbf{v}_{\boldsymbol{\tau}}) - j(\mathbf{u}_{\boldsymbol{\tau}}) \ge (\mathbf{f}, \mathbf{v} - \mathbf{u}) \quad \forall\, \mathbf{v} \in \mathbf{V}, \tag{2.4}$$

$$d(\mathbf{u}, q) = 0 \quad \forall\, q \in Q, \tag{2.5}$$

where the bilinear forms and the barrier term $j(\cdot)$ against slip on Γ_S are defined as

$$a(\mathbf{u}, \mathbf{v}) = \nu(\nabla\mathbf{u}, \nabla\mathbf{v}), \quad d(\mathbf{v}, p) = (\nabla \cdot \mathbf{v}, p) \quad \forall\, \mathbf{u}, \mathbf{v} \in \mathbf{V},\ p \in Q,$$

$$j(\boldsymbol{\eta}) = \int_{\Gamma_S} g\,|\boldsymbol{\eta}|\,\mathrm{d}s \quad \forall\, \boldsymbol{\eta} \in \boldsymbol{\Lambda},$$

along with

$$(p, q) := \int_\Omega p(\mathbf{x})q(\mathbf{x})\,\mathrm{d}\mathbf{x} \quad \forall\, p, q \in L^2(\Omega), \quad (\mathbf{v}, \mathbf{w}) := \int_\Omega \sum_{i=1}^{2} \mathrm{v}_i(\mathbf{x})\mathrm{w}_i(\mathbf{x})\,\mathrm{d}\mathbf{x} \quad \forall\, \mathbf{v}, \mathbf{w} \in \mathbf{Y},$$

$$(\nabla\mathbf{v}, \nabla\mathbf{w}) := \int_\Omega \sum_{i,j=1}^{2} \frac{\partial \mathrm{v}_i}{\partial x_j}\frac{\partial \mathrm{w}_i}{\partial x_j}\,\mathrm{d}\mathbf{x} \quad \forall\, \mathbf{v}, \mathbf{w} \in \mathbf{H}^1(\Omega).$$

Obviously, the forms $a(\cdot,\cdot)$ and $d(\cdot,\cdot)$ are continuous and $j(\cdot)$ is also a continuous functional on $\boldsymbol{\Lambda}$. As a consequence of Korn's inequality ([43]), there exists a constant $\alpha > 0$ such that

$$a(\mathbf{v}, \mathbf{v}) \geq \alpha \|\mathbf{v}\|_{\mathbf{V}}^2 \quad \forall \mathbf{v} \in \mathbf{V}.$$

Existence and uniqueness results to the variational inequality problem (2.4)–(2.5) are proven in [41,44].

Introduce the Lagrangian multiplier $\boldsymbol{\lambda} := -\boldsymbol{\sigma}_{\boldsymbol{\tau}}/g$, then the inequality problem (2.4)–(2.5) is equivalent to the equation problem [42,45,46]: find $(\mathbf{u}, p, \boldsymbol{\lambda}) \in \mathbf{V} \times Q \times \boldsymbol{\Lambda}$ such that

$$a(\mathbf{u}, \mathbf{v}) - d(\mathbf{v}, p) + \langle g\boldsymbol{\lambda}, \mathbf{v}_{\boldsymbol{\tau}}\rangle_{\boldsymbol{\Lambda}} = (\mathbf{f}, \mathbf{v}) \quad \forall\, \mathbf{v} \in \mathbf{V}, \tag{2.6}$$

$$d(\mathbf{u}, q) = 0 \quad \forall\, q \in Q, \tag{2.7}$$

$$|\boldsymbol{\lambda}| \leq 1, \ \boldsymbol{\lambda}\cdot\mathbf{u}_{\boldsymbol{\tau}} = |\mathbf{u}_{\boldsymbol{\tau}}| \ \text{ a.e. on } \Gamma_S. \tag{2.8}$$

Remark 1. (i) Without loss of generality, we take $\nu = 1$. This can be achieved through a scaling of the problem if ν is a constant different from 1.

(ii) In this work, we adopt the $\boldsymbol{\sigma}_{\boldsymbol{\tau}}(\mathbf{u}) = \nu\frac{\partial \mathbf{u}_{\boldsymbol{\tau}}}{\partial \mathbf{n}}$ introduced by Fujita in [41], it is supposed the boundary $\partial\Omega$ is smooth with $\overline{\Gamma}_D \cap \overline{\Gamma}_S = \varnothing$. While in [28,30] and other work, they defined $\boldsymbol{\sigma}_{\boldsymbol{\tau}} = (\mathbb{T}(\mathbf{u}, p)\mathbf{n})_{\boldsymbol{\tau}}$, with $\mathbb{T}(\mathbf{u}, p) = 2\nu\mathbb{D}(\mathbf{u}) - p\mathbb{I}$, $\mathbb{D}(\mathbf{u}) = \frac{1}{2}(\nabla\mathbf{u} + \nabla^t\mathbf{u})$, then the smooth assumption on the boundary is not essential, and $\Gamma_D \cap \Gamma_S = \varnothing$ is applicable.

3. Finite element method

Let $\mathscr{T}_h$ be a regular family of finite element triangulations of the domain Ω into triangles $\{K\}$, and we assume that the partition $\mathscr{T}_h$ is locally quasi-uniform. Let $e = \partial K_i \cap \partial K_j$ $(i \neq j)$ be the common boundary between two elements K_i and K_j in $\mathscr{T}_h$. The diameters of K and e are denoted by h_K and h_e. We will use $\mathscr{E}(K)$ for the set of sides of K, $\mathscr{E}_h^S$ for the subset of the element sides lying on the boundary Γ_S, $\mathscr{E}_h^0$ the set of all interior edges of $\mathscr{T}_h$ and $\mathscr{E}_h = \mathscr{E}_h^0 \cup \mathscr{E}_h^S$. In addition, the patch $\widetilde{K}$ associated with any element K from a partition $\mathscr{T}_h$ consists of all elements sharing at least one vertex with K, i.e., $\widetilde{K} = \mathrm{int}(\cup\{K' \in \mathscr{T}_h : \overline{K}' \cap \overline{K} \neq \emptyset\})$.

To approximate the velocity and pressure, two cases of finite element pairs $\mathbf{P}_2 - P_1$, $\mathbf{P}_{1b} - P_1$ and $\mathbf{P}_1 - P_1$, $\mathbf{P}_1 - P_0$ may be adopted, that is, we employ the following approximation spaces:

Case 1: Stable finite element pairs

$$\mathbf{V}^h := \begin{cases} \mathbf{P}_2 = \{\mathbf{v}_h \in [C(\overline{\Omega})]^2 \cap \mathbf{V},\ \mathbf{v}_h|_K \in [\mathcal{P}_2(K)]^2,\ \forall K \in \mathscr{T}_h\}, \\ \mathbf{P}_{1b} = \{\mathbf{v}_h \in [C(\overline{\Omega})]^2 \cap \mathbf{V},\ \mathbf{v}_h|_K \in [\mathcal{P}_1(K)]^2 \oplus [\mathcal{B}(K)]^2,\ \forall K \in \mathscr{T}_h\}, \end{cases}$$

$$Q_h := P_1 = \{q_h \in C(\overline{\Omega}) \cap Q,\ q_h|_K \in \mathcal{P}_1(K),\ \forall K \in \mathscr{T}_h\}.$$

Case 2: Unstable finite element pairs

$$\mathbf{V}^h := \mathbf{P}_1 = \{\mathbf{v}_h \in [C(\overline{\Omega})]^2 \cap \mathbf{V},\ \mathbf{v}_h|_K \in [\mathcal{P}_1(K)]^2,\ \forall K \in \mathscr{T}_h\},$$

$$Q_h =: \begin{cases} P_1 = \{q_h \in C(\bar{\Omega}) \cap Q,\ q_h|_K \in \mathcal{P}_1(K),\ \forall K \in \mathscr{T}_h\}, \\ P_0 = \{q_h \in Q,\ q_h|_K \in \mathcal{P}_0(K),\ \forall K \in \mathscr{T}_h\}. \end{cases}$$

Here, $\mathcal{P}_k(K)$ is the space of polynomials of degree at most k and $\mathcal{B}(K)$ is the space spanned by the bubble functions on K. The following inf–sup property holds with non-negative constants $\beta, \delta_1, \delta_2$ independent of h [47,48]:

$$\beta\|q\|_0 \leq \sup_{\mathbf{v}\in\mathring{\mathbf{V}}_h} \frac{d(\mathbf{v}, q)}{\|\mathbf{v}\|_1} + \delta_1 Ch\|\nabla q\|_0 + \delta_2 Ch^{1/2}\|[q]\|_0 \quad \forall\, q \in Q_h, \tag{3.1}$$

where $\mathring{\mathbf{V}}_h = \mathbf{H}_0^1(\Omega) \cap \mathbf{V}^h$ and $[q]$ denotes the jump of $q \in P_0$. We have $\delta_1 = \delta_2 = 0$ if $\mathbf{P}_2 - P_1$ and $\mathbf{P}_{1b} - P_1$ are selected, while $\delta_2 = 0$ if $\mathbf{P}_1 - P_1$ is chosen and $\delta_1 = 0$ for $\mathbf{P}_1 - P_0$ finite element pair. Under the unstable situation, we draw into a pressure-stabilizer [35,47,49]

$$G(p, q) = \delta(p - \Pi p, q - \Pi q) \quad \forall\, p, q \in Q_h,$$

with $\delta = 0$ for **Case 1** and $\delta = 1$ for **Case 2**. And Π is an L^2-projection operator:

$$\Pi = \begin{cases} \Pi_1 : L^2(\Omega) \to P_1, & \text{if } Q_h = P_0, \\ \Pi_0 : L^2(\Omega) \to P_0, & \text{if } Q_h = P_1. \end{cases}$$

Now to approximate $\mathbf{V}$, we introduce

$$\mathbf{V}_h = \{\mathbf{v}_h \in \mathbf{V}^h,\ \mathbf{v}_h = 0 \text{ on } \Gamma_D,\ \mathrm{v}_{h\mathbf{n}} = 0 \text{ on } \Gamma_S,\ \forall K \in \mathscr{T}_h\}.$$

The discrete formulation of the variational inequality (2.4)–(2.5) reads: find $(\mathbf{u}_h, p_h) \in \mathbf{V}_h \times Q_h$ such that

$$a(\mathbf{u}_h, \mathbf{v}_h - \mathbf{u}_h) - d(\mathbf{v}_h - \mathbf{u}_h, p_h) + j(\mathbf{v}_{h\boldsymbol{\tau}}) - j(\mathbf{u}_{h\boldsymbol{\tau}}) \geq (\mathbf{f}, \mathbf{v}_h - \mathbf{u}_h) \quad \forall \mathbf{v}_h \in \mathbf{V}_h, \tag{3.2}$$

$$d(\mathbf{u}_h, q_h) + G(p_h, q_h) = 0 \quad \forall q_h \in Q_h, \tag{3.3}$$

This discrete problem has a unique solution [28,33,41]. Analysis of the finite element approximation under stable and unstable finite element pairs of such problems is discussed in [25,28,32,46,50]. For derivation of the a posteriori error estimator, we will need the following finite element approximation to problem (2.6)–(2.8): find $(\mathbf{u}_h, p_h) \in \mathbf{V}_h \times Q_h$ and $\boldsymbol{\lambda}_h \in \boldsymbol{\Lambda}$ such that

$$a(\mathbf{u}_h, \mathbf{v}_h) - d(\mathbf{v}_h, p_h) + \langle g\boldsymbol{\lambda}_h, \mathbf{v}_{h\boldsymbol{\tau}}\rangle_{\boldsymbol{\Lambda}} = (\mathbf{f}, \mathbf{v}_h) \quad \forall \mathbf{v}_h \in \mathbf{V}_h, \tag{3.4}$$

$$d(\mathbf{u}_h, q_h) + G(p_h, q_h) = 0 \quad \forall q_h \in Q_h, \tag{3.5}$$

$$|\boldsymbol{\lambda}_h| \leq 1,\ \boldsymbol{\lambda}_h \cdot \mathbf{u}_{h\boldsymbol{\tau}} = |\mathbf{u}_{h\boldsymbol{\tau}}| \ \text{ a.e. on } \Gamma_S. \tag{3.6}$$

For the arguments of the existence of the Lagrangian multiplier $\boldsymbol{\lambda}_h$ and the equivalence between the inequality problem (3.2)–(3.3) and equality problem (3.4)–(3.6), one can refer to [21,46] to achieve the analogues.

Remark 2. (i) If the integrals $j(\cdot)$ and $\langle g\cdot, \cdot\rangle_{\boldsymbol{\Lambda}}$ on Γ_S in (2.4) and (2.6), respectively, are approximated by trapezoidal or Simpson formulas in (3.2) and (3.4) for the different finite element pairs, it has also been proved that the variational inequality problem (3.2)–(3.3) and the problem (3.4)–(3.6) are equivalent with a discrete subspace $\boldsymbol{\Lambda}_h$ [25,30].

(ii) We work with the stabilized terms based on the L^2-projection for brevity which are parameter free and independent of the mesh size, and for more involved ones see [51].

(iii) If we let $A(\mathbf{u}, p; \mathbf{v}, q) = a(\mathbf{u}, \mathbf{v}) - d(\mathbf{v}, p) + d(\mathbf{u}, q) + G(p, q)$, then there exists a positive constant C independent of h such that [47,49]

$$\sup_{(\mathbf{v},q)\in \mathring{\mathbf{V}}_h \times Q_h} \frac{A(\mathbf{u}, p; \mathbf{v}, q)}{\|\mathbf{v}\|_1 + \|q\|_0} \geq C(\|\mathbf{u}\|_1 + \|p\|_0) \quad \forall (\mathbf{u}, p) \in \mathring{\mathbf{V}}_h \times Q_h.$$

4. A posteriori error estimator of residual type

In this section, we present a residual-type estimator for the error $\mathbf{e} = \mathbf{u} - \mathbf{u}_h$, $\epsilon := p - p_h$ by using the characterizations in terms of the Lagrangian multiplier for the true and discrete solutions. The reliability and efficiency of the residual-type error estimator are shown only for the stable finite element pairs, while the analysis process is also applicable to the unstable finite element pairs $\mathbf{P}_1 - P_1$ and $\mathbf{P}_1 - P_0$, one can refer to [11] where the Stokes equations with Dirichlet boundary condition are studied. For vectors $\mathbf{v}$ and $\mathbf{n}$, let $\mathbf{v} \otimes \mathbf{n}$ denote the matrix whose (i, j)th component is $\mathrm{v}_i \mathrm{n}_j$.

Define interior residuals for each element $K \in \mathscr{T}_h$ by

$$\mathbf{R}_K = \mathbf{f} + \Delta \mathbf{u}_h - \nabla p_h \quad \text{in } K, \tag{4.1}$$

and side residuals for each edge $e \in \mathscr{E}_h$ by

$$\mathbf{R}_e = \begin{cases} -[\nabla \mathbf{u}_h - p_h \mathbb{I}], & \text{if } e \in \mathscr{E}_h^0, \\ -(\mathbb{I} - \mathbf{n}_K \otimes \mathbf{n}_K)\nabla \mathbf{u}_h \mathbf{n}_K - g\boldsymbol{\lambda}_{h\boldsymbol{\tau}} & \text{if } e \in \mathscr{E}_h^S, \end{cases}$$

where the quantity

$$[\nabla \mathbf{u}_h - p_h \mathbb{I}] = \mathbf{n}_{K_1}(\nabla \mathbf{u}_h - p_h \mathbb{I})|_{e\cap K_1} + \mathbf{n}_{K_2}(\nabla \mathbf{u}_h - p_h \mathbb{I})|_{e\cap K_2},$$

represents the jump discontinuity in the approximation to the normal derivative on the side e which separates the neighboring elements K_1 and K_2.

Define a local error estimator by

$$\eta_K^2 = h_K^2 \|\mathbf{R}_K\|_{0,K}^2 + \|\nabla \cdot \mathbf{u}_h\|_{0,K}^2 + \frac{1}{2} \sum_{e\in \mathscr{E}(K)\cap \mathscr{E}_h^0} h_e \|\mathbf{R}_e\|_{0,e}^2 + \sum_{e\in \mathscr{E}(K)\cap \mathscr{E}_h^S} h_e \|\mathbf{R}_e\|_{0,e}^2,$$

and let

$$\eta^2 := \sum_{K\in \mathscr{T}_h} \eta_K^2.$$

4.1. Reliability

Lemma 1. *Let* $(\mathbf{u}, p)$ *and* $(\mathbf{u}_h, p_h)$ *be the solutions of* (2.6)–(2.8) *and* (3.4)–(3.6). *Then*

$$\|\epsilon\|_0 \le C(\eta + \|\mathbf{e}\|_1). \tag{4.2}$$

Proof. Taking an arbitrary $\mathbf{w}_h \in \mathring{\mathbf{V}}_h$ as a test function in (2.6) yields

$$a(\mathbf{u}, \mathbf{w}_h) - d(\mathbf{w}_h, p) = (\mathbf{f}, \mathbf{w}_h). \tag{4.3}$$

Similarly, it follows from (3.4) that

$$a(\mathbf{u}_h, \mathbf{w}_h) - d(\mathbf{w}_h, p_h) = (\mathbf{f}, \mathbf{w}_h). \tag{4.4}$$

By subtraction of (4.3) and (4.4), there holds

$$a(\mathbf{e}, \mathbf{w}_h) - d(\mathbf{w}_h, \epsilon) = 0. \tag{4.5}$$

Let $\mathbf{v}_I \in \mathring{\mathbf{V}}_h$ be the regularized interpolation of $\mathbf{v} \in \mathbf{H}_0^1(\Omega)$. Using integration by parts and (4.5), we have

$$\begin{aligned}
(\nabla\cdot\mathbf{v}, \epsilon) &= (\nabla\cdot(\mathbf{v}-\mathbf{v}_I), \epsilon) + (\nabla\cdot\mathbf{v}_I, \epsilon)\\
&= (\nabla\cdot(\mathbf{v}-\mathbf{v}_I), \epsilon) + (\nabla\mathbf{e}, \nabla\mathbf{v}_I)\\
&= (\nabla\cdot(\mathbf{v}-\mathbf{v}_I), \epsilon) - (\nabla\mathbf{e}, \nabla(\mathbf{v}-\mathbf{v}_I)) + (\nabla\mathbf{e}, \nabla\mathbf{v})\\
&= -\sum_K (\mathbf{f} + \Delta\mathbf{u}_h - \nabla p_h, \mathbf{v}-\mathbf{v}_I)_K - \sum_K \int_{\partial K} (\nabla\mathbf{u}_h - p_h\mathbb{I})\mathbf{n}\cdot(\mathbf{v}-\mathbf{v}_I)\,\mathrm{d}s + (\nabla\mathbf{e}, \nabla\mathbf{v})\\
&\le C\|\mathbf{v}\|_1\Big((\sum_{K\in\mathcal{T}_h} h_K^2\|\mathbf{f} + \Delta\mathbf{u}_h - \nabla p_h\|_{0,K}^2)^{1/2} + (\sum_{e\in\mathscr{E}_h^0} h_e\|[\nabla\mathbf{u}_h - p_h\mathbb{I}]\|_e^2)^{1/2} + \|\mathbf{e}\|_1\Big).
\end{aligned} \tag{4.6}$$

The inf-sup condition (3.1) implies that

$$\|p - p_h\|_0 \le C(\eta + \|\mathbf{e}\|_1).$$

It completes the proof. □

To bound $\|\mathbf{e}\|_1$, we subtract (3.4) from (2.6) with $\mathbf{v} = \mathbf{v}_h \in \mathbf{V}_h$ to get the Galerkin orthogonality relation for the error

$$a(\mathbf{e}, \mathbf{v}_h) - d(\mathbf{v}_h, \epsilon) + \langle g(\boldsymbol{\lambda} - \boldsymbol{\lambda}_h), \mathbf{v}_{h\boldsymbol{\tau}}\rangle_{\boldsymbol{\Lambda}} = 0 \quad \forall\, \mathbf{v}_h \in \mathbf{V}_h. \tag{4.7}$$

For any $\mathbf{v} \in \mathbf{V}$, there holds

$$\begin{aligned}
a(\mathbf{e}, \mathbf{v}) - d(\mathbf{v}, \epsilon) &= a(\mathbf{u}, \mathbf{v}) - d(\mathbf{v}, p) - a(\mathbf{u}_h, \mathbf{v}) + d(\mathbf{v}, p_h)\\
&= (\mathbf{f}, \mathbf{v}) - \langle g\boldsymbol{\lambda}, \mathbf{v}_{\boldsymbol{\tau}}\rangle_{\boldsymbol{\Lambda}} - ((\nabla\mathbf{u}_h, \nabla\mathbf{v}) - (\nabla\cdot\mathbf{v}, p_h)),
\end{aligned} \tag{4.8}$$

where (2.6) is used. Then performing integration by parts over each element and regrouping the terms result in

$$\begin{aligned}
&(\nabla\mathbf{u}_h, \nabla\mathbf{v}) - (\nabla\cdot\mathbf{v}, p_h)\\
&= \sum_K (-\Delta\mathbf{u}_h + \nabla p_h, \mathbf{v})_K + \sum_K \int_{\partial K} (\nabla\mathbf{u}_h - p_h\mathbb{I})\mathbf{n}|_K\cdot\mathbf{v}\,\mathrm{d}s\\
&= \sum_K (-\Delta\mathbf{u}_h + \nabla p_h, \mathbf{v})_K + \int_{\mathscr{E}_h^0} [\nabla\mathbf{u}_h - p_h\mathbb{I}]\cdot\mathbf{v}\,\mathrm{d}s + \int_{\mathscr{E}_h^S} (\mathbb{I} - \mathbf{n}\otimes\mathbf{n})\nabla\mathbf{u}_h\mathbf{n}\cdot\mathbf{v}_{\boldsymbol{\tau}}\,\mathrm{d}s.
\end{aligned} \tag{4.9}$$

Inserting (4.9) into (4.8), with the fact that $\boldsymbol{\lambda}_h = \boldsymbol{\lambda}_{h\boldsymbol{\tau}} + \lambda_{h\mathbf{n}}\mathbf{n}$ and $\lambda_{h\mathbf{n}}\mathbf{n}\cdot\mathbf{v}_{\boldsymbol{\tau}} = 0$, we get

$$\begin{aligned}
&a(\mathbf{e}, \mathbf{v}) - d(\mathbf{v}, \epsilon)\\
&= \sum_K (\mathbf{f} + \Delta\mathbf{u}_h - \nabla p_h, \mathbf{v})_K - \langle g\boldsymbol{\lambda}, \mathbf{v}_{\boldsymbol{\tau}}\rangle_{\boldsymbol{\Lambda}} - \int_{\mathscr{E}_h^0} [\nabla\mathbf{u}_h - p_h\mathbb{I}]\cdot\mathbf{v}\,\mathrm{d}s - \int_{\mathscr{E}_h^S} (\mathbb{I} - \mathbf{n}\otimes\mathbf{n})\nabla\mathbf{u}_h\mathbf{n}\cdot\mathbf{v}_{\boldsymbol{\tau}}\,\mathrm{d}s\\
&= \sum_K (\mathbf{f} + \Delta\mathbf{u}_h - \nabla p_h, \mathbf{v})_K - \int_{\mathscr{E}_h^0} [\nabla\mathbf{u}_h - p_h\mathbb{I}]\cdot\mathbf{v}\,\mathrm{d}s - \langle g(\boldsymbol{\lambda} - \boldsymbol{\lambda}_h), \mathbf{v}_{\boldsymbol{\tau}}\rangle_{\boldsymbol{\Lambda}}\\
&\quad - \int_{\mathscr{E}_h^S} \big(g\boldsymbol{\lambda}_{h\boldsymbol{\tau}} + (\mathbb{I} - \mathbf{n}\otimes\mathbf{n})\nabla\mathbf{u}_h\mathbf{n}\big)\cdot\mathbf{v}_{\boldsymbol{\tau}}\,\mathrm{d}s.
\end{aligned}$$

Thus,

$$a(\mathbf{e}, \mathbf{v}) - d(\mathbf{v}, \epsilon) + \langle g(\boldsymbol{\lambda} - \boldsymbol{\lambda}_h), \mathbf{v}_{\boldsymbol{\tau}}\rangle_{\boldsymbol{\Lambda}} = \sum_K (\mathbf{R}_K, \mathbf{v})_K + \int_{\mathscr{E}_h^0} \mathbf{R}_e\cdot\mathbf{v}\,\mathrm{d}s + \int_{\mathscr{E}_h^S} \mathbf{R}_e\cdot\mathbf{v}_{\boldsymbol{\tau}}\,\mathrm{d}s. \tag{4.10}$$

Note that this residual equation together with (4.7) implies the orthogonality relation:

$$\sum_K (\mathbf{R}_K, \mathbf{v}_h)_K + \int_{\mathscr{E}_h^0} \mathbf{R}_e \cdot \mathbf{v}_h \, ds + \int_{\mathscr{E}_h^S} \mathbf{R}_e \cdot \mathbf{v}_{h\tau} \, ds = 0 \quad \forall \mathbf{v}_h \in \mathbf{V}_h. \tag{4.11}$$

It follows from (2.8) and (3.6) that

$$\begin{aligned}\int_{\mathscr{E}_h^S} g(\boldsymbol{\lambda} - \boldsymbol{\lambda}_h)(\mathbf{u}_{h\boldsymbol{\tau}} - \mathbf{u}_{\boldsymbol{\tau}}) \, ds &= \int_{\mathscr{E}_h^S} g\boldsymbol{\lambda}\mathbf{u}_{h\boldsymbol{\tau}} \, ds - \int_{\mathscr{E}_h^S} g\boldsymbol{\lambda}\mathbf{u}_{\boldsymbol{\tau}} \, ds - \int_{\mathscr{E}_h^S} g\boldsymbol{\lambda}_h\mathbf{u}_{h\boldsymbol{\tau}} \, ds + \int_{\mathscr{E}_h^S} g\boldsymbol{\lambda}_h\mathbf{u}_{\boldsymbol{\tau}} \, ds \\ &\le \int_{\mathscr{E}_h^S} g|\mathbf{u}_{h\boldsymbol{\tau}}| \, ds - \int_{\mathscr{E}_h^S} g|\mathbf{u}_{\boldsymbol{\tau}}| \, ds - \int_{\mathscr{E}_h^S} g|\mathbf{u}_{h\boldsymbol{\tau}}| \, ds + \int_{\mathscr{E}_h^S} g|\mathbf{u}_{\boldsymbol{\tau}}| \, ds = 0,\end{aligned}$$

and also from (2.7) that

$$d(\mathbf{u}, \epsilon) = 0.$$

Taking $\mathbf{v} = \mathbf{e}$ in (4.10), we derive

$$a(\mathbf{e}, \mathbf{e}) - d(\mathbf{e}, \epsilon) \le a(\mathbf{e}, \mathbf{e}) - d(\mathbf{e}, \epsilon) + \langle g(\boldsymbol{\lambda} - \boldsymbol{\lambda}_h), \mathbf{e}_{\boldsymbol{\tau}} \rangle_{\boldsymbol{\Lambda}} = \sum_K (\mathbf{R}_K, \mathbf{e})_K + \int_{\mathscr{E}_h^0} \mathbf{R}_e \cdot \mathbf{e} \, ds + \int_{\mathscr{E}_h^S} \mathbf{R}_e \cdot \mathbf{e}_{\boldsymbol{\tau}} \, ds.$$

By (4.11),

$$a(\mathbf{e}, \mathbf{e}) - d(\mathbf{e}, \epsilon) \le \sum_K \int_K \mathbf{R}_K \cdot (\mathbf{e} - \mathbf{v}_h) \, d\mathbf{x} + \int_{\mathscr{E}_h^0} \mathbf{R}_e \cdot (\mathbf{e} - \mathbf{v}_h) \, ds + \int_{\mathscr{E}_h^S} \mathbf{R}_e \cdot (\mathbf{e}_{\boldsymbol{\tau}} - \mathbf{v}_{h\boldsymbol{\tau}}) \, ds \quad \forall \mathbf{v}_h \in \mathbf{V}_h.$$

Then,

$$\begin{aligned}\|\mathbf{e}\|_1^2 &= a(\mathbf{e}, \mathbf{e}) - d(\mathbf{e}, \epsilon) + d(\mathbf{e}, \epsilon) = a(\mathbf{e}, \mathbf{e}) - d(\mathbf{e}, \epsilon) - d(\mathbf{u}_h, \epsilon) \\ &\le \sum_K (\mathbf{R}_K, \mathbf{e})_K + \int_{\mathscr{E}_h^0} \mathbf{R}_e \cdot \mathbf{e} \, ds + \int_{\mathscr{E}_h^S} \mathbf{R}_e \cdot \mathbf{e}_{\boldsymbol{\tau}} \, ds - d(\mathbf{u}_h, \epsilon) \\ &\le \sum_K (\mathbf{R}_K, \mathbf{e} - \mathbf{v}_h)_K + \int_{\mathscr{E}_h^0} \mathbf{R}_e \cdot (\mathbf{e} - \mathbf{v}_h) \, ds + \int_{\mathscr{E}_h^S} \mathbf{R}_e \cdot (\mathbf{e}_{\boldsymbol{\tau}} - \mathbf{v}_{h\boldsymbol{\tau}}) \, ds + \|\nabla \cdot \mathbf{u}_h\|_0 \|\epsilon\|_0.\end{aligned}$$

Let $\mathcal{L}_h : \mathbf{V} \to \mathbf{V}_h$ be the locally regularized interpolant operator introduced in [52]. Set $\mathbf{v}_h = \mathcal{L}_h\mathbf{e}$ and apply the Cauchy–Schwarz inequality, yielding

$$\begin{aligned}&\|\mathbf{e}\|_1^2 \\ &\le \sum_K \int_K \mathbf{R}_K \cdot (\mathbf{e} - \mathcal{L}_h\mathbf{e}) \, d\mathbf{x} + \int_{\mathscr{E}_h^0} \mathbf{R}_e \cdot (\mathbf{e} - \mathcal{L}_h\mathbf{e}) \, ds + \int_{\mathscr{E}_h^S} \mathbf{R}_e \cdot (\mathbf{e}_{\boldsymbol{\tau}} - \mathcal{L}_h\mathbf{e}_{h\boldsymbol{\tau}}) \, ds + \|\nabla \cdot \mathbf{u}_h\|_0 \|\epsilon\|_0 \\ &\le \sum_K \|\mathbf{R}_K\|_{0,K} \|\mathbf{e} - \mathcal{L}_h\mathbf{e}\|_{0,K} + \sum_{e \in \mathscr{E}_h^0} \|\mathbf{R}_e\|_{0,e} \|\mathbf{e} - \mathcal{L}_h\mathbf{e}\|_{0,e} + \sum_{e \in \mathscr{E}_h^S} \|\mathbf{R}_e\|_{0,e} \|\mathbf{e}_{\boldsymbol{\tau}} - \mathcal{L}_h\mathbf{e}_{\boldsymbol{\tau}}\|_{0,e} + \|\nabla \cdot \mathbf{u}_h\|_0 \|\epsilon\|_0 \\ &\le C\|\mathbf{e}\|_1 \left\{ \sum_K h_K^2 \|\mathbf{R}_K\|_{0,K}^2 + \frac{1}{2} \sum_{e \in \mathscr{E}(K) \cap \mathscr{E}_h^0} h_e \|\mathbf{R}_e\|_{0,e}^2 + \sum_{e \in \mathscr{E}(K) \cap \mathscr{E}_h^S} h_e \|\mathbf{R}_e\|_{0,e}^2 \right\}^{1/2} + C\|\nabla \cdot \mathbf{u}_h\|_0 (\eta + \|\mathbf{e}\|_1).\end{aligned}$$

Therefore,

$$\|\mathbf{e}\|_1^2 \le C\eta^2. \tag{4.12}$$

In actual computations, the terms on the right side of (4.12) are regrouped as a summation of the contributions from each element $K \in \mathscr{T}_h$. We summarize the above result in the form of a theorem.

Theorem 2. *Let $(\boldsymbol{u}, p)$ and $(\boldsymbol{u}_h, p_h)$ be the unique solution of (2.4)–(2.5) and (3.2)–(3.3), respectively. Then we have*

$$\|\mathbf{u} - \mathbf{u}_h\|_1 + \|p - p_h\|_0 \le C\eta, \tag{4.13}$$

where the constant C depends only on the domain Ω and the minimal angle condition, and is independent of the mesh-size.

4.2. Efficiency of the a posteriori error estimator

We follows Verfürth [5,12] to discuss an upper bound of the error estimator, which will use the canonical bubble functions constructed for each element $K \in \mathscr{T}_h$ and each side $e \in \mathscr{E}_h$. Let ξ_1, ξ_2 and ξ_3 be the barycentric coordinates on K, the interior bubble function φ_K is defined by

$$\varphi_K = \begin{cases} 27\xi_1\xi_2\xi_3 & \text{in } K, \\ 0 & \text{in } \Omega \setminus K. \end{cases}$$

For each side $e \in \mathscr{E}_h^0$, we can analogously define an edge bubble function φ_e. Let K_1 and K_2 be two elements sharing e, and let $\omega_e = K_1 \cup K_2$ be the union of the elements K_1 and K_2. Denote by $\xi_1^{K_i}$ and $\xi_2^{K_i}$ the barycentric coordinates in K_i, $i = 1, 2$, that are associated with the two ends of e. Then the edge bubble function is

$$\varphi_e = \begin{cases} 4\xi_1^{K_i}\xi_2^{K_i} & \text{in } K_i, \\ 0 & \text{in } \Omega \setminus \omega_e. \end{cases}$$

In particular, for the side $e \in \mathscr{E}_h^S$, $\omega_e = K$ and then the edge bubble function is $\varphi_e = 4\xi_1\xi_2$.

Lemma 3 ([3,53,54]). (1) *There exist positive constants C_m^1 and C_m^2, depending only on m, such that for any polynomial $\boldsymbol{\phi} \in \boldsymbol{L}^2(K)$ with degree at most m,*

$$C_m^1 \|\boldsymbol{\phi}\|_{0,K}^2 \le \int_K \varphi_K \boldsymbol{\phi}^2 \, d\mathbf{x} \le \|\boldsymbol{\phi}\|_{0,K}^2, \tag{4.14}$$

$$\|\varphi_K \boldsymbol{\phi}\|_{1,K} \le C_m^2 h_K^{-1} \|\boldsymbol{\phi}\|_{0,K}. \tag{4.15}$$

(2) *There exist positive constants C_m^3 and C_m^4, depending only on m, such that for any polynomial $\psi \in L^2(e)$ with degree at most m,*

$$C_m^3 \|\psi\|_{0,e}^2 \le \int_e \varphi_e \psi^2 \, ds \le \|\psi\|_{0,e}^2, \tag{4.16}$$

$$C_m^4 \|\psi\|_{0,e} \le h_e^{-1/2} \|\varphi_e P\psi\|_{0,\omega_e} + h_e^{1/2} \|\varphi_e P\psi\|_{1,\omega_e} \le \|\psi\|_{0,e}, \tag{4.17}$$

where $P : C(e) \to C(K)$, $K \in \mathscr{T}_h$, $e \in \mathscr{E}_h$ is an extension operator, which maps $\mathcal{P}_k(e)$ into $\mathcal{P}_k(K)$.

Let $\widetilde{\mathbf{f}}$ be a piecewise constant function whose value in $K \in \mathscr{T}_h$ equals the mean value of $\mathbf{f}$ on K. Following an argument similar to that from [3,5,11], we get a local bound for the residual type error estimator.

Lemma 4. *There exists a generic constant $C > 0$ such that,*

$$h_K \|\mathbf{f} + \Delta \mathbf{u}_h - \nabla p_h\|_{0,K} \le C(\|\mathbf{e}\|_{1,K} + \|\epsilon\|_{0,K} + h_K \|\mathbf{f} - \widetilde{\mathbf{f}}\|_{0,K}), \tag{4.18}$$

$$h_e^{1/2} \|[\nabla \mathbf{u}_h - p_h \mathbb{I}]\|_{0,e} \le C(h_e \|\mathbf{f} - \widetilde{\mathbf{f}}\|_{0,\omega_e} + \|\mathbf{e}\|_{1,\omega_e} + \|\epsilon\|_{0,\omega_e}), \tag{4.19}$$

$$\|\nabla \cdot \mathbf{u}_h\|_{0,K} \le C \|\mathbf{e}\|_{1,K}. \tag{4.20}$$

Up to this circumstance, the control of the element residual $\mathbf{R}_K$, the interior side residual $\mathbf{R}_e$, the divergence term $\|\nabla \cdot \mathbf{u}_h\|_{0,K}$ had been shown. Finally, we consider those sides e lying on Γ_S and let γ be the element whose boundary contains e.

From the definition of $\mathbf{R}_e$ on $e \in \mathscr{E}_h^S$, we realize that $\mathbf{R}_e \in \mathbf{V}$. Let $P(\mathbf{R}_e) \in [\mathcal{P}_K]^2$ be an approximation of $\mathbf{R}_e$, which referred to [53] also keeps the property in $\mathbf{V}$. Now it follows from Lemma 3 that

$$\|\mathbf{R}_e\|_{0,e}^2 \le C \int_e \varphi_e P(\mathbf{R}_e)^2 \, ds. \tag{4.21}$$

According to $\mathbf{v} \in \mathbf{V}$ and $\mathbf{v} = v_{\mathbf{n}}\mathbf{n} + \mathbf{v}_{\boldsymbol{\tau}}$, the residual equation (4.10) can be rewritten as

$$a(\mathbf{e}, \mathbf{v}) - d(\mathbf{v}, \epsilon) + \langle g(\boldsymbol{\lambda} - \boldsymbol{\lambda}_h), \mathbf{v}_{\boldsymbol{\tau}} \rangle_{\boldsymbol{\Lambda}} = \sum_K (\mathbf{R}_K, \mathbf{v})_K + \int_{\mathscr{E}_h} \mathbf{R}_e \cdot \mathbf{v} \, ds.$$

Let $\mathbf{v}_h = \varphi_e P(\mathbf{R}_e) \in \mathbf{V}$, extend this function to the whole domain by zero value outside γ, with this choice of $\mathbf{v}_h$, the above equation becomes

$$a(\mathbf{e}, \varphi_e P(\mathbf{R}_e)) - d(\varphi_e P(\mathbf{R}_e), \epsilon_h) = \int_\gamma \mathbf{R}_\gamma^K \varphi_e P(\mathbf{R}_e) \, d\mathbf{x} + \int_e \mathbf{R}_e \varphi_e P(\mathbf{R}_e) \, ds + \int_e g(\boldsymbol{\lambda}_h - \boldsymbol{\lambda}) \big(\varphi_e P(\mathbf{R}_e)\big)_{\boldsymbol{\tau}} \, ds,$$

which leads to

$$\begin{aligned} \int_e \varphi_e P(\mathbf{R}_e)^2 \, ds = & \int_e \varphi_e P(\mathbf{R}_e)(P(\mathbf{R}_e) - \mathbf{R}_e) \, ds + a(\mathbf{e}, \varphi_e P(\mathbf{R}_e)) - d(\varphi_e P(\mathbf{R}_e), \epsilon_h) \\ & - \int_\gamma \mathbf{R}_\gamma^K \varphi_e P(\mathbf{R}_e) \, d\mathbf{x} - \int_e g(\boldsymbol{\lambda}_h - \boldsymbol{\lambda}) \big(\varphi_e P(\mathbf{R}_e)\big)_{\boldsymbol{\tau}} \, ds, \end{aligned} \tag{4.22}$$

where $\mathbf{R}_\gamma^K$ is the interior residual on the element γ. Applying the Cauchy–Schwarz inequality and Lemma 3, the first three terms on the right side of (4.22) can be bounded. Using (4.21), we can obtain

$$\begin{aligned} \|\mathbf{R}_e\|_{0,e}^2 \le & C \left(\|\mathbf{R}_e\|_{0,e} \|P(\mathbf{R}_e) - \mathbf{R}_e\|_{0,e} + h_e^{-1/2} (\|\mathbf{e}\|_{1,K} + \|\epsilon\|_{0,K}) \|\mathbf{R}_e\|_{0,e} + h_e^{1/2} \|\mathbf{R}_e\|_{0,e} \|\mathbf{R}_\gamma^K\|_{0,\gamma} \right) \\ & + \int_e g(\boldsymbol{\lambda}_h - \boldsymbol{\lambda}) \big(\varphi_e P(\mathbf{R}_e)\big)_{\boldsymbol{\tau}} \, ds. \end{aligned}$$

Multiplying both sides of this inequality by h_e and summing over all sides $e \in \mathscr{E}_h^S$, we get

$$\sum_{e\in\mathscr{E}_h^S} h_e\|\mathbf{R}_e\|_{0,e}^2 \le C\sum_{e\in\mathscr{E}_h^S} h_e^{1/2}\|\mathbf{R}_e\|_{0,e} h_e^{1/2}\|P(\mathbf{R}_e)-\mathbf{R}_e\|_{0,e} + C\sum_{e\in\mathscr{E}_h^S} h_e^{1/2}(\|\mathbf{e}\|_{1,K}+\|\epsilon\|_{0,K})\|\mathbf{R}_e\|_{0,e} + C\sum_{e\in\mathscr{E}_h^S} h_e^{1/2}\|\mathbf{R}_e\|_{0,e}\, h_e\|\mathbf{R}_\gamma^K\|_{0,\gamma} + |R_{h,\Gamma_S}|, \tag{4.23}$$

where

$$R_{h,\Gamma_S} = \int_{\mathscr{E}_h^S} g(\boldsymbol{\lambda}_h-\boldsymbol{\lambda})\, h_e\left(\varphi_e P(\mathbf{R}_e)\right)_{\boldsymbol{\tau}}\, \mathrm{d}s.$$

We can bound R_{h,Γ_S} as follows

$$|R_{h,\Gamma_S}| \le \sum_{e\in\mathscr{E}_h^S} h_e^{1/2}\|g(\boldsymbol{\lambda}-\boldsymbol{\lambda}_h)\|_{0,e}\, h_e^{1/2}\|\varphi_e P(\mathbf{R}_e)\|_{0,e} \le C\Big(\sum_{e\in\mathscr{E}_h^S} h_e\|\boldsymbol{\lambda}-\boldsymbol{\lambda}_h\|_{0,e}^2\Big)^{1/2}\Big(\sum_{e\in\mathscr{E}_h^S} h_e\|\mathbf{R}_e\|_{0,e}^2\Big)^{1/2}.$$

Using this bound in (4.23) and applying the Cauchy–Schwarz inequality lead to

$$\sum_{e\in\mathscr{E}_h^S} h_e\|\mathbf{R}_e\|_{0,e}^2 \le C\Big(\sum_{e\in\mathscr{E}_h^S} h_e\|P(\mathbf{R}_e)-\mathbf{R}_e\|_{0,e}^2 + \sum_{e\in\mathscr{E}_h^S} h_e^2\|\mathbf{R}_\gamma^K\|_{0,\gamma}^2 + (\|\mathbf{e}\|_1+\|\epsilon\|_0)^2 + \sum_{e\in\mathscr{E}_h^S} h_e\|\boldsymbol{\lambda}-\boldsymbol{\lambda}_h\|_{0,e}^2\Big). \tag{4.24}$$

Summarizing (4.18), (4.20) with all elements $K \in \mathscr{T}_h$, (4.19) with all $e \in \mathscr{E}_h^0$, then combining them with (4.24), we have

$$\sum_{K\in\mathscr{T}_h} \eta_K^2 \le C\Big((\|\mathbf{e}_h\|_1+\|\epsilon_h\|_0)^2 + \sum_{e\in\mathscr{E}_h^S} h_e\|\boldsymbol{\lambda}-\boldsymbol{\lambda}_h\|_{0,e}^2 + \sum_{e\in\mathscr{E}_h^S} h_e\|P(\mathbf{R}_e)-\mathbf{R}_e\|_{0,e}^2 + \sum_{K\in\mathscr{T}_h} h_K^2\|\mathbf{f}-\widetilde{\mathbf{f}}\|_{0,K}^2\Big). \tag{4.25}$$

Since $\nabla\mathbf{u}_h\mathbf{n}$ on e and $P(\mathbf{R}_e)$ are all polynomials. Therefore, the term $\|P(\mathbf{R}_e)-\mathbf{R}_e\|_{0,e}$ on the right side of (4.25) can be replaced by $\|\mathbf{f}-\widetilde{\mathbf{f}}\|_{0,K}$ and $\|\boldsymbol{\lambda}_h-\boldsymbol{\lambda}_{h,e}\|_{0,e}$, with discontinuous piecewise polynomial approximations $\widetilde{\mathbf{f}}$ and $\boldsymbol{\lambda}_{h,e}$.

Theorem 5. *Let η be defined as in (4.1). Then we have*

$$\eta^2 \le C\Big((\|\mathbf{u}-\mathbf{u}_h\|_1+\|p-p_h\|_0)^2 + \sum_{e\in\mathscr{E}_h^S} h_e\|\boldsymbol{\lambda}-\boldsymbol{\lambda}_h\|_{0,e}^2 + \sum_{K\in\mathscr{T}_h} h_K^2\|\mathbf{f}-\widetilde{\mathbf{f}}\|_{0,K}^2 + \sum_{e\in\mathscr{E}_h^S} h_e\|\boldsymbol{\lambda}_h-\boldsymbol{\lambda}_{h,e}\|_{0,e}^2\Big),$$

with discontinuous piecewise polynomial approximations $\widetilde{\mathbf{f}}$, $\boldsymbol{\lambda}_{h,e}$ of $\mathbf{f}$, $\boldsymbol{\lambda}_h$.

Remark 3. A residual error estimator is investigated for the variational inequality governed by the Stokes equations, the analytical techniques used here can also be extended to other types of the posteriori error estimators, e.g. the gradient recovery type. Besides, the process of proof can also be applicable to the unstable finite element pairs or other numerical methods.

5. Numerical results

In this section, we give numerical examples on the two-dimensional problem. First we explain two algorithms: one is an adaptive algorithm for refinement, and the other is the iterative algorithm for solving the variational inequality.

5.1. Algorithms

Adaptive implementation. The local a posteriori error estimator η_K defined in Section 4 can be used to provide algorithms for local grid refinement. we apply the local refinement by "Maximum Strategy" which is described briefly below; for more detail, the reader is referred to [10,55–57]. Adaptive finite element solutions are computed as follows.

Step 1. Start with an initial triangular mesh $\mathscr{T}_h$.

Step 2. Compute the solution $(\mathbf{u}_h^{ad}, p_h^{ad}) \in \mathbf{V}_h \times Q_h$ and error estimator η_K on each triangle.

Step 3. Let the maximum error $\eta_{max} = \max \eta_K$. For a fixed given threshold $\theta \in (0, 1)$ (e.g. $\theta = 0.35$), if $\eta_K > \theta\eta_{max}$, mark the triangle K for refinement.

Step 4. Perform refinement by the newest node bisection method [55,56] and obtain a new triangulation $\mathscr{T}_h$.

Step 5. Return to Step 2.

In the computation of the indicator η_K in Step 2, we make use of the multiplier $\boldsymbol{\lambda}_h$ defined on $\Gamma_S \subset \partial\Omega$. In what follows we briefly describe how $\boldsymbol{\lambda}_h$ can be recovered from the numerical solution $(\mathbf{u}_h, p_h)$ using (3.4); more details are given in [21].

We now show how to recover the Lagrangian multiplier $\boldsymbol{\lambda}_h = (\lambda_h^1, \lambda_h^2)^T$, which can be a piecewise constant, a piecewise linear or a quadratic polynomial, denoted by $\boldsymbol{\lambda}_{h,\alpha}$, $\alpha = 0, 1, 2$. Denote by $\{\mathbf{a}_j\}_{j=1}^m$ the nodes of the partition $\mathscr{T}_h$ belonging to

$\overline{\Gamma}_S$. Let $\{\varphi_j\}_{j=1}^m$ be the basis functions corresponding to the nodes $\{\mathbf{a}_j\}$ and χ_j be the characteristic functions of the intervals $\{I_j\}$ belonging to $\overline{\Gamma}_S$ which is defined as follows: I_j is the intersection of Γ_S and the segment joining the midpoints of edges sharing $\mathbf{a}_j$ as a common point. We define a piecewise constant function

$$\boldsymbol{\lambda}_{h,0} = \begin{pmatrix} \sum_{j=1}^m \lambda_{h,0}^{1,j}\chi_j \\ \sum_{j=1}^m \lambda_{h,0}^{2,j}\chi_j \end{pmatrix},$$

or the piecewise linear or quadratic function

$$\boldsymbol{\lambda}_{h,\alpha} = \begin{pmatrix} \sum_{j=1}^m \lambda_{h,\alpha}^{1,j}\varphi_j \\ \sum_{j=1}^m \lambda_{h,\alpha}^{2,j}\varphi_j \end{pmatrix}, \quad \text{with } \alpha = 1, 2.$$

Let $n_1 = \dim(\mathbf{V}_h)$, $n_2 = \dim(Q_h)$. Denote by $\mathbb{A}$ the standard $n_1 \times n_1$ stiffness matrix, $\mathbb{B}_\kappa (\kappa = 1, 2)$ the standard $n_1 \times n_2$ stiffness matrix and by $\boldsymbol{\ell}_1, \boldsymbol{\ell}_2 \in \mathcal{R}^{n_1}$ the standard load vector for the Stokes problems. $\mathbb{M}_1, \mathbb{M}_2 \in \mathcal{R}^m \times \mathcal{R}^m$ are sparse matrices. Let $\mathbf{u} = (\mathbb{u}_1, \mathbb{u}_2)^T \in \mathcal{R}^{2n_1}$, $\mathbb{p} \in \mathcal{R}^{n_2}$ be the nodal value vectors of the finite element solution $\mathbf{u}_h, p_h$. Then the algebraic representation of (3.4)–(3.5) becomes

$$\begin{bmatrix} \mathbb{A} & \mathbb{0} & \mathbb{B}_1 \\ \mathbb{0} & \mathbb{A} & \mathbb{B}_2 \\ -\mathbb{B}_1^T & -\mathbb{B}_2^T & \mathbb{0} \end{bmatrix} \begin{bmatrix} \mathbb{u}_1 \\ \mathbb{u}_2 \\ \mathbb{p} \end{bmatrix} + \begin{bmatrix} g\mathbb{M}_1 & \mathbb{0} \\ \mathbb{0} & g\mathbb{M}_2 \end{bmatrix} \begin{bmatrix} \lambda_{h,\alpha}^1 \\ \lambda_{h,\alpha}^2 \end{bmatrix} = \begin{bmatrix} \boldsymbol{\ell}_1 \\ \boldsymbol{\ell}_2 \\ \mathbf{0} \end{bmatrix}.$$

We denote by $\mathbb{u}_{\kappa,s}$ the subvector of $\mathbb{u}_\kappa$, containing the nodal values at the vertices $\{\mathbf{a}_j\}_{j=1}^m \subset \overline{\Gamma}_S$. We can write $\mathbb{u}_\kappa = (\mathbb{u}_{\kappa,i}, \mathbb{u}_{\kappa,s})^T \in \mathcal{R}^{n_1-m} \times \mathcal{R}^m$ by assuming that the components of $\mathbb{u}_{\kappa,s}$ and $\mathbb{p}$ are listed last. We also similarly split $\boldsymbol{\ell}_\kappa$ to $\boldsymbol{\ell}_{\kappa,i}$ and $\boldsymbol{\ell}_{\kappa,s}$. This decomposition yields a block structure for $\mathbb{A}$ and $\mathbb{B}_\kappa$,

$$\mathbb{A} = \begin{bmatrix} \mathbb{A}_{ii} & \mathbb{A}_{is} \\ \mathbb{A}_{si} & \mathbb{A}_{ss} \end{bmatrix}, \quad \mathbb{B}_\kappa = \begin{bmatrix} \mathbb{B}_{\kappa,in_2} & \mathbb{B}_{\kappa,sn_2} \end{bmatrix}.$$

Then (3.4)–(3.5) are equivalent to

$$\begin{aligned} \mathbb{A}_{ii}\mathbb{u}_{\kappa,i} + \mathbb{A}_{is}\mathbb{u}_{\kappa,s} + \mathbb{B}_{\kappa,in_2}\,\mathbb{p} &= \boldsymbol{\ell}_{\kappa,i}, \\ \mathbb{A}_{si}\mathbb{u}_{\kappa,i} + \mathbb{A}_{ss}\mathbb{u}_{\kappa,s} + g\mathbb{M}_\kappa\lambda_{h,\alpha}^\kappa &= \boldsymbol{\ell}_{\kappa,s}. \end{aligned}$$

Once the numerical solution $(\mathbf{u}_h, p_h)$ is computed, from the second relation we see that

$$\lambda_{h,\alpha}^\kappa = g^{-1}\mathbb{M}_\kappa^{-1}(\boldsymbol{\ell}_{\kappa,s} - \mathbb{A}_{si}\mathbb{u}_{\kappa,i} - \mathbb{A}_{ss}\mathbb{u}_{\kappa,s}), \quad \kappa = 1, 2.$$

Uzawa algorithm. Based on the above preparations, we give the iterative algorithm to compute the numerical solutions on each layer of partition, for $\alpha = 0$, 1 or 2.

(1) Choose an initial value $\boldsymbol{\lambda}_{h,\alpha}^{(0)}$.

(2) Solve the following linear Stokes system to obtain $(\mathbf{u}_h^{(n)}, p_h^{(n)})$, $n = 1, 2, \ldots,$

$$\begin{cases} a(\mathbf{u}_h^{(n)}, \mathbf{v}_h) - d(\mathbf{v}_h, p_h^{(n)}) = (\mathbf{f}, \mathbf{v}_h) - \langle g\boldsymbol{\lambda}_{h,\alpha}^{(n-1)}, \mathbf{v}_{h\boldsymbol{\tau}}\rangle_{\boldsymbol{\Lambda}}, \\ \qquad\qquad d(\mathbf{u}_h^{(n)}, q_h) = 0. \end{cases}$$

(3) Update the multiplier $\boldsymbol{\lambda}_{h,\alpha}^{(n)}$ by the relations

$$\boldsymbol{\lambda}_{h,\alpha}^{(n),j} = g^{-1}\mathbb{M}^{-1}(\boldsymbol{\ell}_s - \mathbb{A}_{si}\mathbb{u}_i - \mathbb{A}_{ss}\mathbb{u}_s), \quad \text{with } \boldsymbol{\lambda}_{h,\alpha}^{(n)} = \sum_{j=1}^m \boldsymbol{\lambda}_{h,\alpha}^{(n),j}\varphi_{j,\alpha}.$$

and

$$\boldsymbol{\lambda}_{h,\alpha}^{(n)} = \max\{\min\{\boldsymbol{\lambda}_{h,\alpha}^{(n)}, \mathbf{1}\}, -\mathbf{1}\},$$

where φ represents the basis functions corresponding to the Lagrangian multiplier.

(4) Return to (2) until the tolerance error is satisfied.

5.2. Examples

We now present two numerical examples to show the robustness and reliability of the a posteriori error estimator.

Example 1. Let $\Omega = (0, 1)^2$, whose boundary is split into the slip boundary $\Gamma_S = (0, 1) \times \{1\}$ and the Dirichlet boundary $\Gamma_D = \partial\Omega \setminus \Gamma_S$. The exact solution $(\mathbf{u}, p)$ satisfies (2.1)–(2.2) is

$$\mathbf{u}(x, y) = \begin{pmatrix} 10x^2(x-1)^2y(y-1)(2y-1) \\ -10x(x-1)(2x-1)y^2(y-1)^2 \end{pmatrix}, \quad p(x, y) = 10(2x-1)(2y-1). \tag{5.1}$$

Table 1
Values of the Lagrangian multiplier λ_h for the uniform and adaptive meshes on Γ_S.

g	0.1		0.5		1.0		$\lvert\boldsymbol{\sigma}_{\boldsymbol{\tau}}\rvert$	
λ_h^1	0.0		0.0		0.0		0.0	
x	λ_h^{un}	λ_h^{ad}	λ_h^{un}	λ_h^{ad}	λ_h^{un}	λ_h^{ad}	λ_h^{un}	λ_h^{ad}
0.0	0.0	0.0	0.0	0.0	0.0	0.0	0.0	0.0
0.1	−0.93	−0.94	−0.27	−0.21	−0.15	−0.17	−1.0	−1.0
0.2	−1.0	−1.0	−0.64	−0.61	−0.38	−0.34	−1.0	−1.0
0.3	−1.0	−1.0	−0.95	−0.96	−0.57	−0.50	−1.0	−1.0
0.4	−1.0	−1.0	−1.0	−1.0	−0.69	−0.68	−1.0	−1.0
0.5	−1.0	−1.0	−1.0	−1.0	−0.81	−0.95	−1.0	−1.0
0.6	−1.0	−1.0	−1.0	−1.0	−0.69	−0.70	−1.0	−1.0
0.7	−1.0	−1.0	−0.95	−0.95	−0.57	−0.50	−1.0	−1.0
0.8	−1.0	−1.0	−0.64	−0.63	−0.38	−0.35	−1.0	−1.0
0.9	−0.93	−0.94	−0.26	−0.21	−0.15	−0.17	−1.0	−1.0
1.0	0.0	0.0	0.0	0.0	0.0	0.0	0.0	0.0

The external force $\mathbf{f}$ can be found from (2.1),

$$\mathbf{f}(x,y)=\begin{pmatrix} -20\nu(6x^2-6x+1)y(y-1)(2y-1)-60\nu(x^2(x-1)^2)(2y-1)+20(2y-1) \\ 60\nu(2x-1)y^2(2y-1)^2+20\nu x(x-1)(2x-1)(6y^2-6y+1)+20(2x-1) \end{pmatrix}.$$

It is easy to verify that $\mathbf{u}$ satisfies the boundary condition (2.3) on Γ_D and Γ_S. We can specify $\boldsymbol{\sigma}_{\boldsymbol{\tau}}$ as follows:

$$\boldsymbol{\sigma}_{\boldsymbol{\tau}}=\begin{pmatrix} 10x^2(x-1)^2 \\ 0 \end{pmatrix} \quad \text{on} \quad \Gamma_S.$$

Moreover, the position friction function g can be chosen as $|\boldsymbol{\sigma}_{\boldsymbol{\tau}}|$ on the slip boundary Γ_S by (2.3). By a direct computation, we find that

$$\max_{\Gamma_S}|\boldsymbol{\sigma}_{\boldsymbol{\tau}}|=\max_{0\le x\le 1}|10x^2(x-1)^2|=0.625.$$

Now, instead of the adhesive boundary condition, we impose the slip boundary condition on Γ_S, for a fixed function g. Then it can be seen that

$$\begin{cases} g(\mathbf{x})>|\boldsymbol{\sigma}_{\boldsymbol{\tau}}(\mathbf{x})| \text{ for all nodes } \mathbf{x}\in\Gamma_S \Rightarrow (5.1) \text{ remains the solution} \Rightarrow \text{No-slip occurs.} \\ g(\mathbf{x}_0)=|\boldsymbol{\sigma}_{\boldsymbol{\tau}}(\mathbf{x}_0)| \text{ for some nodes } \mathbf{x}_0\in\Gamma_S \Rightarrow (5.1) \text{ is no longer a solution} \Rightarrow \text{Slip occurs.} \end{cases}$$

In particular, for a constant g,

$$\begin{cases} g>0.625 \Rightarrow (5.1) \text{ remains the solution} \Rightarrow \text{No-slip occurs.} \\ g\le 0.625 \Rightarrow (5.1) \text{ is no longer a solution} \Rightarrow \text{Slip occurs.} \end{cases}$$

The slip and non-slip phenomena are clearly observed in Figs. 1 and 2 for different friction functions g. Table 1 shows the values of the multiplier $\boldsymbol{\lambda}_h$ on x-axis corresponding to Figs. 1, 2. These results are selected only for the $\mathbf{P}_2-P_1$ finite element pair since the results are similar for the two cases of finite element pairs ($\mathbf{P}_2-P_1$, $\mathbf{P}_{1b}-P_1$ and $\mathbf{P}_1-P_1$, $\mathbf{P}_1-P_0$), as well as on a 16×16 grid for uniform partitions, on an initial 8×8 grid after 4 times iteration for adaptive mesh. Moreover, for $\mathbf{P}_2-P_1$, we choose the quadratic polynomials as the basis functions of $\boldsymbol{\lambda}_h$, while for the finite element pairs $\mathbf{P}_1-P_1$, $\mathbf{P}_1-P_0$, we choose the linear polynomials as the basis functions of $\boldsymbol{\lambda}_h$.

In fact, when g is a constant, slip phenomena ($\mathbf{u}_{h\boldsymbol{\tau}}\neq 0$) take place on Γ_S for $0.1, 0.5$, whereas no slip is observed for $g=1.0$. While g is a fixed function, if $g(\mathbf{x}_0)$ is bigger than $|\boldsymbol{\sigma}_{\boldsymbol{\tau}}(\mathbf{x}_0)|$, no slip occurs along the top boundary of the computational domain, and slip phenomena appear at the positions where the values of $g(\mathbf{x}_0)$ are less than $|\boldsymbol{\sigma}_{\boldsymbol{\tau}}(\mathbf{x}_0)|$, and the degree of slip occurrence is closely related to the value of the friction function g. These phenomena can also be further verified by the values of $\boldsymbol{\lambda}_h$ in Table 1.

Fig. 3 provides the errors $\|\mathbf{u}-\mathbf{u}_h^{un}\|_1$, $\|p-p_h^{un}\|_0$ and $\|\mathbf{u}-\mathbf{u}_h^{ad}\|_1$, $\|p-p_h^{ad}\|_0$ under the stable finite element pair $\mathbf{P}_2-P_1$ and unstable finite element pairs $\mathbf{P}_1-P_1$, $\mathbf{P}_1-P_0$. The numerical solution corresponding to $h=1/64$ is taken as the "exact" solution $\mathbf{u}$ when slip occurs.

Example 2 (*Simulation of a Blood Flow Model*)**.** This example studies a two-dimensional simplified model of hemokinesis in an arterial vessel whose wall may have an arterial stenosis [58–60]. We assume that the blood flow is a viscous Newtonian flow, and its governing equations are the incompressible stationary Stokes equations. The geometric model is set up and two types of computational domain are displayed in Fig. 4. Blood flows into the vessel from the left entrances and both of the inlets and outlets are labeled. Set the diameter of the main vessel as 2, the length as 12. For the setting shown in Fig. 4(b), a half-square stenosis is attached on the wall of the vessel and the outlet of the flow area is assumed far away from the stenosis.

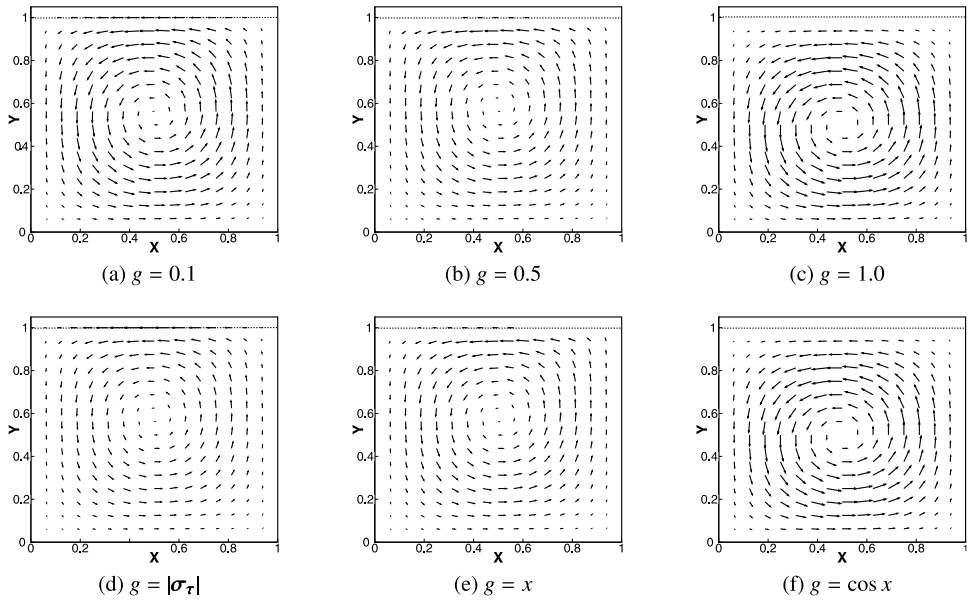

(a) $g = 0.1$ (b) $g = 0.5$ (c) $g = 1.0$

(d) $g = |\boldsymbol{\sigma_\tau}|$ (e) $g = x$ (f) $g = \cos x$

Fig. 1. Velocity field in Ω with different friction function g under uniform meshes.

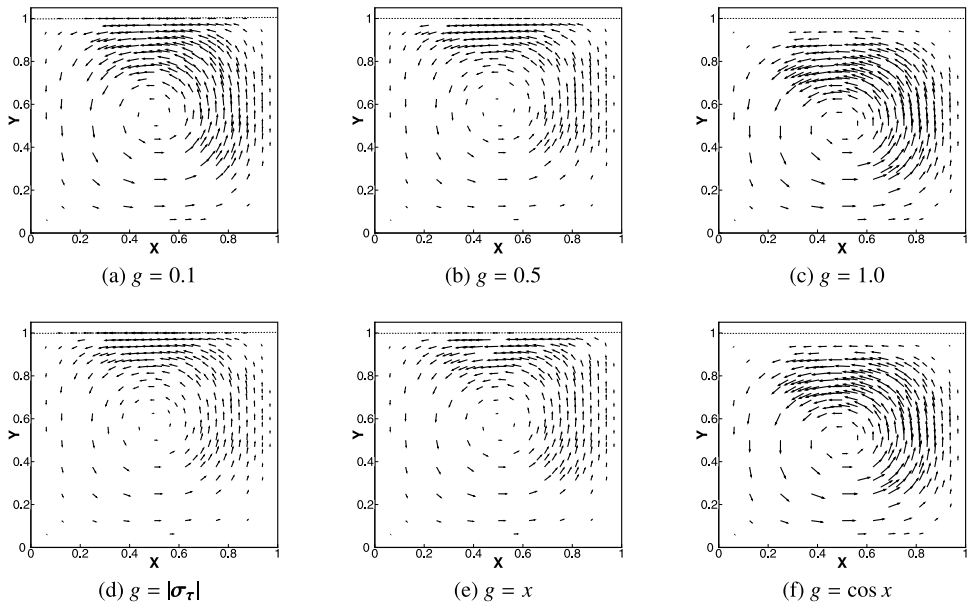

(a) $g = 0.1$ (b) $g = 0.5$ (c) $g = 1.0$

(d) $g = |\boldsymbol{\sigma_\tau}|$ (e) $g = x$ (f) $g = \cos x$

Fig. 2. Velocity field in Ω with different friction function g under adaptive meshes.

We set $h = 1/8$ as the size for the initial unified grid. The inflow velocities are: $u_x = 4 - 4(1-y)^2$, $u_y = 0$, We set the frictional function $g = |\boldsymbol{\sigma_\tau}|$, 4.0, 10. And the velocity $U = (u_{hx}^2 + u_{hy}^2)^{1/2}$. The stable $\mathbf{P}_2 - P_1$ finite element pair is employed and the basis function of $\boldsymbol{\lambda}_h$ is chosen as quadratic polynomials. All the results are selected after 4 times refinement of the initial mesh.

From the compared velocities and contours of pressure in Figs. 5 and 6, one can see that slip phenomena occur when the friction function $g = |\boldsymbol{\sigma_\tau}|$ and $g = 4.0$, while for $g = 10$ no slip phenomenon takes place: the values of velocity along the bottom approach 0 when no slip exists (Figs. 5, 6: (c)), while those in horizontal direction along the upper and lower bottom are no longer 0 except at the entrance (Figs. 5, 6: (a)(b)).

For Domain I, fluid smoothly flows to the outlet and the pressures along the bottom decline in a straight line under $g = 10$. While under $g = |\boldsymbol{\sigma_\tau}|, g = 4.0$, the fluid changes near the entrance and then smoothly flows out (Fig. 7); we can

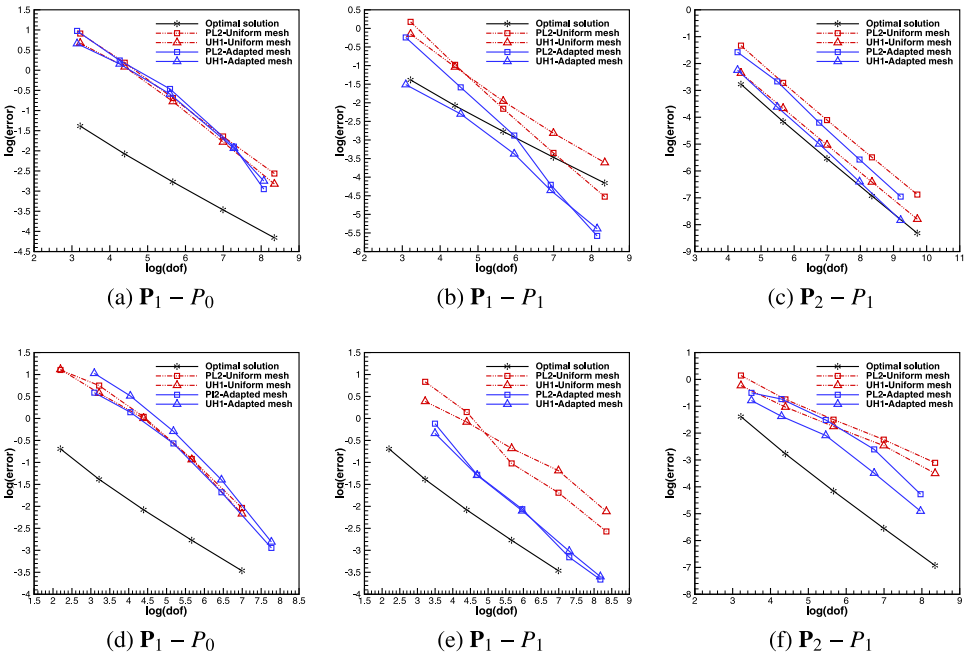

(a) $\mathbf{P}_1 - P_0$ (b) $\mathbf{P}_1 - P_1$ (c) $\mathbf{P}_2 - P_1$

(d) $\mathbf{P}_1 - P_0$ (e) $\mathbf{P}_1 - P_1$ (f) $\mathbf{P}_2 - P_1$

Fig. 3. Error bounds of $\|\mathbf{u} - \mathbf{u}^{un}\|_1$ (Δ), $\|\mathbf{u} - \mathbf{u}^{ad}\|_1$ (Δ) and $\|p - p^{un}\|_0$ (□), $\|p - p^{ad}\|_0$ (□) under $g = 1.0$ (top) and $g = |\boldsymbol{\sigma}_\tau|$ (bottom) for different finite element pairs.

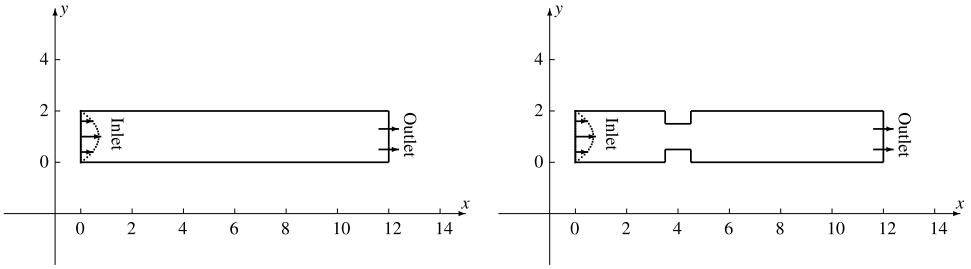

(a) Domain I: without a stenosis (b) Domain II: with a stenosis

Fig. 4. Geometric domain of the vascular model.

also see the pressure along the bottom violently ascends when cross a point, it decreases almost linearly, which is also consistent with the velocity.

For Domain II, when the stenosis exists, flow separation regions begin to appear and the low speed areas are forming, which lead to the eddies (Figs. 6, 8). When there is no slip, the eddies appear at the four corners and the speed in the horizontal and vertical directions are both zero; while the slip phenomena occur (Fig. 6: (a)(b)), the values of velocity in horizontal direction along the bottom are non-vanishing, only the vertical component of velocity vanished, and one observation is that the eddies only appear at the backward of the stenosis, the low speed area become smaller, in addition, the slip regions decrease with the smaller of the friction function g. For the pressure along the upper and lower boundaries, which changes sharply concentrated in the position of a stenosis of the vessel, and at other places, they show more gentle. Meanwhile, the pressure gradient of the main vessel along the local stenosis near the wall is also large (Fig. 6: (d)(e)(f)).

In summary, when the stenosis on the wall of the blood vessel exists, the blood platelets and fibrinogen more easily deposit at the low speed regions, and lower shear stress of the wall in the separation areas makes the accumulation of material around the vessel walls, which can hardly be carried off by the flowing blood. However, with the occurrence of slip phenomenon, the low speed regions reduced, which may help us to design the artificial blood vessel for drag reduction, and further to reduce the risk of arteriosclerosis.

6. Conclusion

We propose a residual type a posteriori error estimator for a variational inequality problem under the stable ($\mathbf{P}_2 - P_1$, $\mathbf{P}_{1b} - P_1$) and unstable ($\mathbf{P}_1 - P_1$, $\mathbf{P}_1 - P_0$) finite element pairs, which is governed by the stationary Stokes equations with

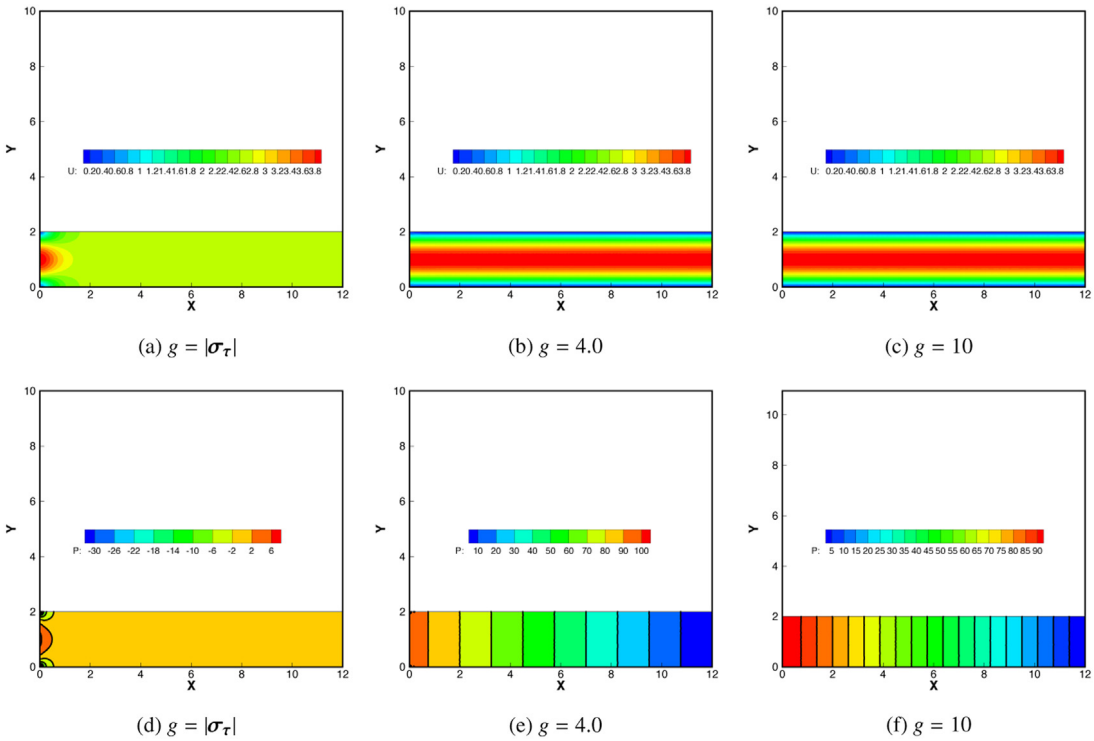

(a) $g = |\boldsymbol{\sigma}_{\boldsymbol{\tau}}|$ (b) $g = 4.0$ (c) $g = 10$

(d) $g = |\boldsymbol{\sigma}_{\boldsymbol{\tau}}|$ (e) $g = 4.0$ (f) $g = 10$

Fig. 5. The results for velocity ((a), (b), (c)) and pressure ((d), (e), (f)) under different friction function g for Domain I.

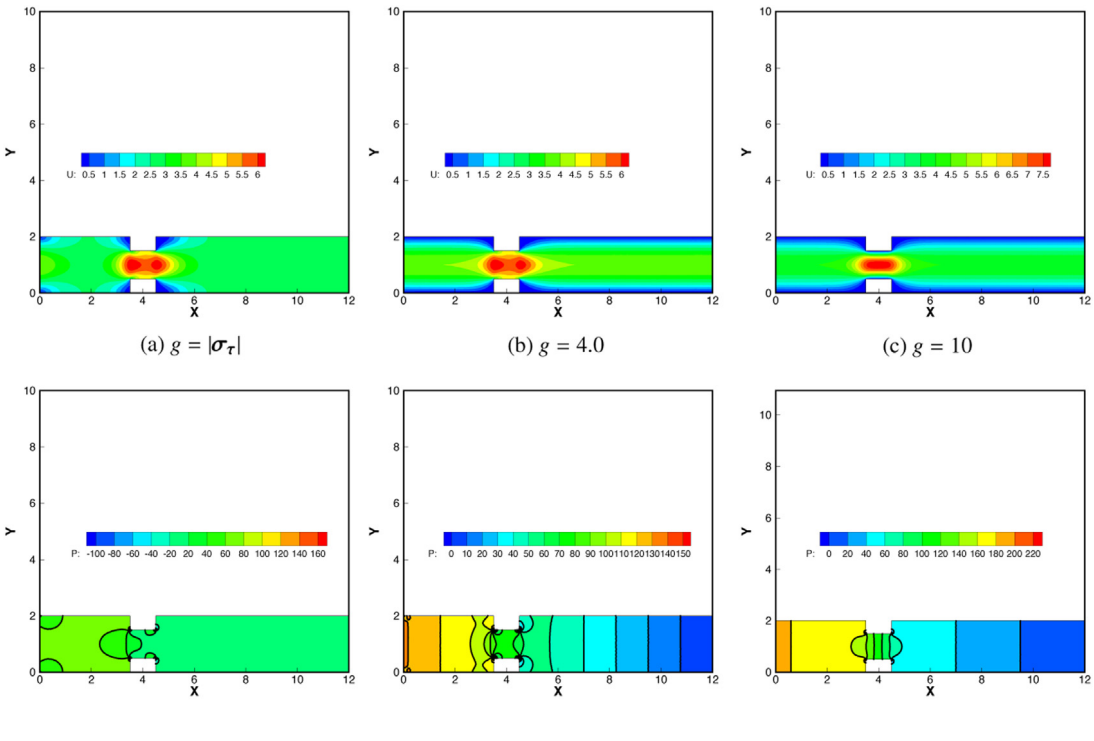

(a) $g = |\boldsymbol{\sigma}_{\boldsymbol{\tau}}|$ (b) $g = 4.0$ (c) $g = 10$

(d) $g = |\boldsymbol{\sigma}_{\boldsymbol{\tau}}|$ (e) $g = 4.0$ (f) $g = 10$

Fig. 6. The results for velocity ((a), (b), (c)) and pressure ((d), (e), (f)) under different friction function g for Domain II.

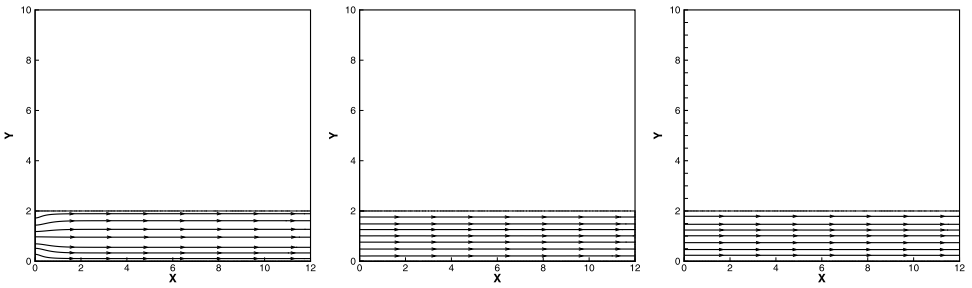

(a) $g = |\boldsymbol{\sigma}_\tau|$ (b) $g = 4.0$ (c) $g = 10$

Fig. 7. The streamlines in Domain I under different friction function.

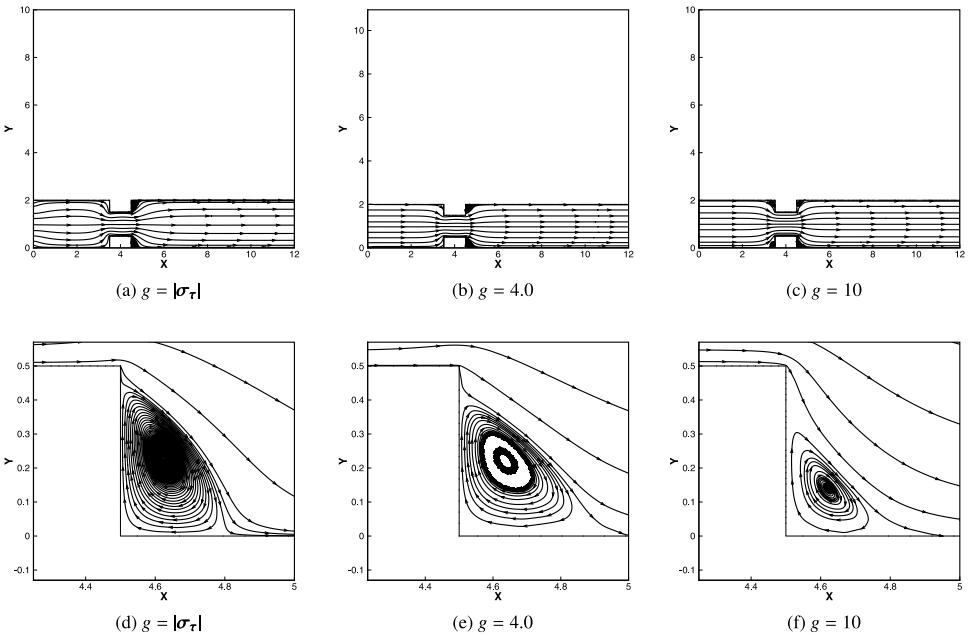

(a) $g = |\boldsymbol{\sigma}_\tau|$ (b) $g = 4.0$ (c) $g = 10$

(d) $g = |\boldsymbol{\sigma}_\tau|$ (e) $g = 4.0$ (f) $g = 10$

Fig. 8. The streamlines in Domain II and local magnified graphs under different friction function.

a nonlinear slip boundary condition of friction type. We prove the reliability by separately estimating the error bounds of velocity and pressure. With the help of canonical bubble functions, we evaluate the efficiency of the global estimator according to the polynomial properties of the numerical quantities, where two discontinuous piecewise polynomial approximations $\widetilde{\mathbf{f}}$ and $\boldsymbol{\lambda}_{h,e}$ are involved. The presented numerical tests demonstrate the reliability and efficiency of the posteriori error estimator. Furthermore, the theoretical technique in this work can be extended to other variational inequality problems, e.g. Navier–Stokes equations with a nonlinear slip or leak boundary condition of friction type.

Acknowledgments

The authors would like to thank Dr. Takahito Kashiwabara and Dr. Guanyu Zhou for the discussions. They also thank the anonymous reviewers for the constructive comments and suggestions.

References

[1] I. Babuška, W.C. Rheinboldt, A posteriori error estimates for the finite element method, Internat. J. Numer. Methods Engrg. 12 (1978) 1597–1615.
[2] I. Babuška, W.C. Rheinboldt, Error estimates for adaptive finite element computations, SIAM J. Numer. Anal. 15 (4) (1978) 736–754.
[3] M. Ainsworth, J.T. Oden, A Posteriori Error Estimation in Finite Element Analysis, Wiley, Chichester, 2000.
[4] I. Babuška, T. Strouboulis, The Finite Element Method and Its Reliability, Oxford University Press, 2001.
[5] R. Verfürth, A Posteriori Error Estimation Techniques for Finite Element Methods, first ed., in: Oxford Science Publications, Oxford University Press, NewYork, 2013.
[6] M. Ainsworth, J.T. Oden, A posteriori error estimators for Stokes and Oseen's equations, SIAM J. Numer. Anal. 17 (1997) 228–246.

[7] R. Bank, B. Welfert, A posteriori error estimators for Stokes problem, SIAM J. Numer. Anal. 28 (1991) 591–623.
[8] W. Doerfler, M. Ainsworth, Reliable a posteriori error control for non-conforming finite element approximation of Stokes flow, Math. Comp. 74 (2005) 1599–1619.
[9] F. Nobile, A Posteriori Error Estimates for the Finite Element Approximation of the Stokes Problem, TICAM Report, 03-13(April), 2003.
[10] J.P. Wang, Y.Q. Wang, X. Ye, A robust nummerical method for Stokes equations based on divergence-free H(div) finite element methods, SIAM J. Sci. Comput. 31 (4) (2009) 2784–2802.
[11] J.P. Wang, Y.Q. Wang, X. Ye, A posteriori error estimate for stabilized finite element methods for the Stokes equations, Int. J. Numer. Anal. Model. 9 (1) (2012) 1–16.
[12] R. Verfürth, A posteriori error estimators for the Stokes equations, Numer. Math. 55 (2) (1989) 309–325.
[13] R. Verfürth, A posteriori error estimators for the Stokes equations ii. non-conforming discretizations, Numer. Math. 60 (1991) 235–249.
[14] L.N. Song, H.Y. Su, X.L. Feng, Recovery-based error estimator for stabilized finite element method for the stationary Navier–Stokes problem, SIAM J. Sci. Comput. 38 (6) (2016) A3758–A3772.
[15] D. Braess, C. Carstensen, H.W. Ronald, Convergence analysis of a conforming adaptive finite element method for an obstacle problem, Numer. Math. 107 (3) (2007) 455–471.
[16] Z. Chen, R.H. Nochetto, Residual type a posteriori error estimates for elliptic obstacle problems, Numer. Math. 84 (2000) 527–548.
[17] R. Kornhuber, A posteriori error estimators for the elliptic variational inequalities, Comput. Math. Appl. 31 (1996) 49–60.
[18] R.H. Nochetto, K.G. Siebert, A. Veeser, Pointwise a posteriori error control for elliptic obstacle probelm, Numer. Math. 95 (2003) 163–195.
[19] A. Veeser, Efficient and reliable a posteriori error estimators for elliptic obstacle problem, SIAM J. Numer. Anal. 95 (2003) 163–195.
[20] N.N. Yan, A posteriori error estimators of gradient recovery type for elliptic obstacle problem, Adv. Comput. Math. 15 (2001) 333–362.
[21] V. Bostan, W. Han, A posteriori error analysis for finite element solutions of a frictional contact problem, Comput. Methods Appl. Mech. Eng. 195 (2006) 1252–1274.
[22] F. Wang, W. Han, Another view for a posteriori error estimates for variational inequalities of the second kind, Appl. Numer. Math. 72 (2013) 225–233.
[23] F. Wang, W. Han, J. Eichholz, X.L. Cheng, A posteriori error estimates for discontinuous Galerkin methods of obstacle problems, Nonlinear Anal. RWA 22 (2015) 664–679.
[24] F.F. Jing, W. Han, W.J. Yan, F. Wang, Discontinuous Galerkin finite element methods for stationary Navier-Stokes problem with a nonlinear slip boundary condition of friction type, J. Sci. Comput. 76 (2) (2018) 888–912.
[25] F.F. Jing, J. Li, Z. Chen, Stabilized finite element methods for a blood flow model of arterosclerosis, Numer. Methods Partial Differential Equations 31 (2015) 2063–2079.
[26] F.F. Jing, J. Li, Z. Chen, W.J. Yan, Discontinuous Galerkin methods for the incompressible flow with nonlinear leak boundary conditions of friction type, Appl. Math. Lett. 73 (2017) 113–119.
[27] F.F. Jing, J. Li, Z. Chen, Z.H. Zhang, Numerical analysis of a characteristic stabilized finite element method for the time-dependent Navier-Stokes equations with nonlinear slip boundary conditions, J. Comput. Appl. Math. 320 (2017) 43–60.
[28] T. Kashiwabara, On a finite element approximation of the Stokes equations under a slip boundary condition of the friction type, Jpn. J. Ind. Appl. Math. 30 (2013) 227–261.
[29] T. Kashiwabara, On a strong solution of the non-stationary Navier-Stokes equations under slip or leak boundary conditions of friction type, J. Differ. Equ. 254 (2013) 756–778.
[30] T. Kashiwabara, Finite element method for Stokes equations under leak boundary condition of friction type, SIAM J. Numer. Anal. 51 (4) (2013) 2445–2469.
[31] T. Kashiwabara, I. Oikawa, G.Y. Zhou, Penalty method with P1/P1 finite element approximation for the Stokes equations under the slip boundary condition, Numer. Math. 134 (4) (2016) 705–740.
[32] Y. Li, K.T. Li, Locally stabilized finite element method for the Stokes problem with nonlinear slip boundary conditions, J. Comput. Math. 28 (6) (2010) 826–836.
[33] Y. Li, K.T. Li, Pressure projection stabilized finite element method for Stokes problem with nonlinear slip boundary conditions, J. Comput. Appl. Math. 235 (6) (2011) 3673–3682.
[34] G.Y. Zhou, T. Kashiwabara, I. Oikawa, Penalty method for the stationary Navier–Stokes problems under the slip boundary condition, J. Sci. Comput. 68 (1) (2016) 339–374.
[35] J. Li, F.F. Jing, Z. Chen, X.L. Lin, A priori and a posteriori estimates of stabilized mixed finite volume methods for the incompressible flow arising in arteriosclerosis, J. Comput. Appl. Math. 363 (2020) 35–52.
[36] F. Wang, M. Ling, W. Han, F.F. Jing, Adaptive discontinuous Galerkin methods for solving an incompressible Stokes flow problem with slip boundary condition of frictional type, J. Comput. Appl. Math. 371 (2020) http://dx.doi.org/10.1016/j.cam.2019.112700.
[37] L.N. Song, Y.R. Hou, Z. Cai, Recovery-based error estimator for stabilized finite element methods for the Stokes equation, Comput. Methods Appl. Mech. Engrg. 272 (2014) 1–16.
[38] O. Zienkiewicz, J. Zhu, The superconvergence patch recovery and a posteriori error estimates, Part I: The recovery technique, Internat. J. Numer. Methods Engrg. 33 (1992) 1331–1364.
[39] O. Zienkiewicz, J. Zhu, The superconvergence patch recovery and a posteriori error estimates, Part II: Error estimates and adaptivity, Internat. J. Numer. Methods Engrg. 33 (1992) 1365–1382.
[40] H. Fujita, Flow Problems with Unilateral Boundary Conditions, College de France, Lecons, 1993.
[41] H. Fujita, A mathematical analysis of motions of viscous incompressible fluid under leak or slip boundary conditions, RIMS Kokyuroku 88 (1994) 199–216.
[42] H. Fujita, H. Kawarada, A. Sasamoto, Analysis and Numerical Approaches to Stationary Flow Problms Wth Leak and Slip Boundary Conditions, in: Lecture Notes in Numer. Appl. Anal., vol. 14, Kinokuniya, Tokyo, 1995, pp. 17–31.
[43] V. Girault, P.A. Raviart, Finite Element Methods for Navier–Stokes Equations. Theory and Algorithms, in: Springer Series in Computational Mathematics, vol. 5, Springer-Verlag, Berlin, 1986.
[44] N. Saito, On the Stokes equations with the leak and slip boundary conditions of friction type: regularity of solutions, Publ. Res. Inst. Math. Sci. 40 (2004) 345–383.
[45] R. Glowinski, Numerical Methods of Nonlinear Variational Problems, Springer-Verlag, New-York, 1984.
[46] Y. Li, K.T. Li, Uzawa iteration method for Stokes type variational inequality of the second kind, Acta Math. Appl. Sin. 17 (2011) 303–316.
[47] P.B. Bochev, C.R. Dohrmann, M.D. Gunzburger, Stabilization of low-order mixed finite element for the Stokes equations, SIAM J. Numer. Anal. 44 (2006) 82–101.
[48] D. Silvester, Stabilised mixed finite element methods, in: Incompressible Flow and the Finite Element Method, Wiley, New York, 1998, pp. 533–549.
[49] J. Li, Y.N. He, A stabilized finite element method based on two local Gauss integrations for the Stokes equations, J. Comput. Appl. Math. 214 (1) (2008) 58–65.

[50] Y. Li, K.T. Li, Pressure projection stabilized finite element method for Navier-Stokes equations with nonlinear slip boundary conditions, Computing 87 (2010) 113–133.
[51] L.P. Franca, R. Stenberg, Error analysis of some Galerkin least squares methods for the elesticity equations, SIAM J. Numer. Anal. 28 (1991) 1680–1697.
[52] C. Bernardi, V. Girault, A local regularization operator for triangular and quadrilateral finite elements, SIAM J. Numer. Anal. 35 (1998) 1893–1916.
[53] R. Verfürth, A posteriori error estimation and adaptive mesh-refinement techniques, J. Comput. Appl. Math. 50 (1994) 67–83.
[54] R. Verfürth, A Review of a Posteriori Error Estimation and Adaptive Mesh-Refinement Techniques, in: Teubner Skripten zur Numerik, B.G. Willey-Teubner, Stuttgart, 1996.
[55] W.F. Mitchell, Unified Multilevel Adaptive Finite Element Methods for Elliptic Problems (Ph.D. dissertation), University of Illinois at Urbana-Champaign, 1988.
[56] E.G. Sewell, Automatic Generation of Triangulations for Piecewise Polynomial Approximation (Ph.D. dissertation), Purdue University, 1972.
[57] J.P. Wang, Y.Q. Wang, X. Ye, Unified a posterriori error estimator for finite element methods for the Stokes equations, Int. J. Numer. Anal. Model. 10 (3) (2013) 551–570.
[58] L. Cai, Y.H. Wang, H. Gao, et al., A mathematical model for active contraction in healthy and failing myocytes and left ventricles, PLoS One 2 (4) (2017).
[59] A.K. Politis, G.P. Stavropoulos, M.N. Christolis, et al., Numerical modeling of simulated blood in idealized composite arterial coronary grafts: steady state simulations, J. Biomech. 40 (2007) 1125–1136.
[60] X.Q. Shen, J.J. Jia, S.F. Zhu, et al., The time-dependent generalized membrane shell model and its numerical computation, Comput. Methods Appl. Mech. Engrg. 344 (2019) 54–70.